Measurement of the *CP*-nonconserving decay, $K_L^0 \to 2\pi^0$

C. A. Rey
*Department of Physics, University of Notre Dame, Notre Dame, Indiana 46556**

R. J. Cence, B. D. Jones,† S. I. Parker, V. Z. Peterson, and V. J. Stenger,
Department of Physics and Astronomy, University of Hawaii, Honolulu, Hawaii 96822‡

R. W. Kenney, I. R. Linscott,§ and W. P. Oliver‖
Lawrence Berkeley Laboratory, University of California, Berkeley, California 94720‡

(Received 27 May 1975)

The rate of the *CP*-nonconserving decay $K_L^0 \to 2\pi^0$ has been measured using a monoenergetic K beam and a nearly-4π-solid-angle detector system employing lead-plate spark chambers and shower counters. Final results based on a detailed analysis of the complete data set are given. The branching ratio of $K_L^0 \to 2\pi^0$ is determined relative to three different normalizations, $K_L^0 \to 3\pi^0$, $K_L^0 \to$ all charged decay modes, and $K_L^0 \to K_S^0$ using a beryllium regenerator. From the $K_L^0 \to 2\pi^0$ rate we find the *CP*-nonconserving parameter $|\eta_{00}|^2 = [14.1 \pm 1.9(\text{stat}) \pm 1.5\ (\text{syst})] \times 10^{-6}$.

I. INTRODUCTION

Since the discovery[1] in 1964 of the decay $K_L^0 \to \pi^+\pi^-$, an extensive search for evidence of *CP* nonconservation in other physical processes has been made.[2] So far *CP*-nonconservation effects have been seen only in three classes of experiments on the neutral K system: (1) measurements of the decay rates of $K_L^0 \to \pi^+\pi^-$ and $K_L^0 \to \pi^0\pi^0$, (2) measurements of the interference effects between the 2π decays of the K_L^0 and K_S^0, and (3) measurements of the charge asymmetry in the leptonic decays of the K_L^0.

We measured the rate of the decay $K_L^0 \to 2\pi^0$ relative to the known rate of $K_L^0 \to 3\pi^0$. The measurement was difficult because the $2\pi^0$ rate is only about 1% of the $3\pi^0$ rate. In addition the neutral nature of the decay chain $K_L^0 \to \pi^0$'s $\to \gamma$'s makes it difficult to obtain much accurate information on the initial and final states. We separated the $3\pi^0$ background from the $2\pi^0$ events principally by observing five or more converted γ rays in a high-efficiency large-solid-angle detection system. The remaining separation was based on the kinematic differences between $2\pi^0$ and $3\pi^0$ four-shower events. The calibrations of the apparatus necessary to evaluate this separation were obtained by direct measurements.

II. GENERAL PLAN OF EXPERIMENT

The design and arrangement of the experimental apparatus was such as to produce an approximately monoenergetic beam of K_L^0 mesons which decayed in flight within a nearly 4π solid-angle γ-ray detection system. The layout of the experimental apparatus[3] is shown in Fig. 1.

To create K_L^0 mesons of known energy, a momentum-analyzed π^- beam from the Bevatron was directed to a 1.2-m-long liquid hydrogen target. The momentum spectrum of the π^- beam was chosen to maximize K^0 production from the reaction $\pi^- p \to \Lambda^0 K^0$ while limiting the contamination of K^0's from the reaction $\pi^- p \to \Sigma^0 K^0$ to only a few percent. Charged particles leaving the hydrogen target were swept out by two bending magnets, leaving a neutral beam of forward-going neutrons, K^0's, and γ rays. The γ rays were filtered from the neutral beam by 10 cm of lead placed 1.8 m downstream from the hydrogen target.

After the lead filter the remaining K_L^0's and neutrons drifted downstream a distance of 3.3 m where they entered a 1-m^3 air-filled decay volume which was enclosed by a five-sided cube of lead-plate spark chambers. The geometry for detecting γ rays was enhanced by placing a tunnel consisting of lead-lucite Čerenkov counters at the entrance to the spark-chamber array.

γ rays from the decay of a K_L^0 meson into neutral pions were detected by two banks of scintillation-Čerenkov trigger counters placed in the downstream spark chamber. Charged particles entering the spark chambers were identified by scintillation counters covering the walls of the decay volume. The signature for a K_L^0 decay into a neutral final state was taken to be (1) a beam particle entering the liquid hydrogen target and not continuing along the beam, (2) no charged particles detected in the lead filter, (3) two γ-ray showers in the downstream spark chamber separated by a minimum distance of 28 cm, and (4) no charged particles entering the spark chambers.

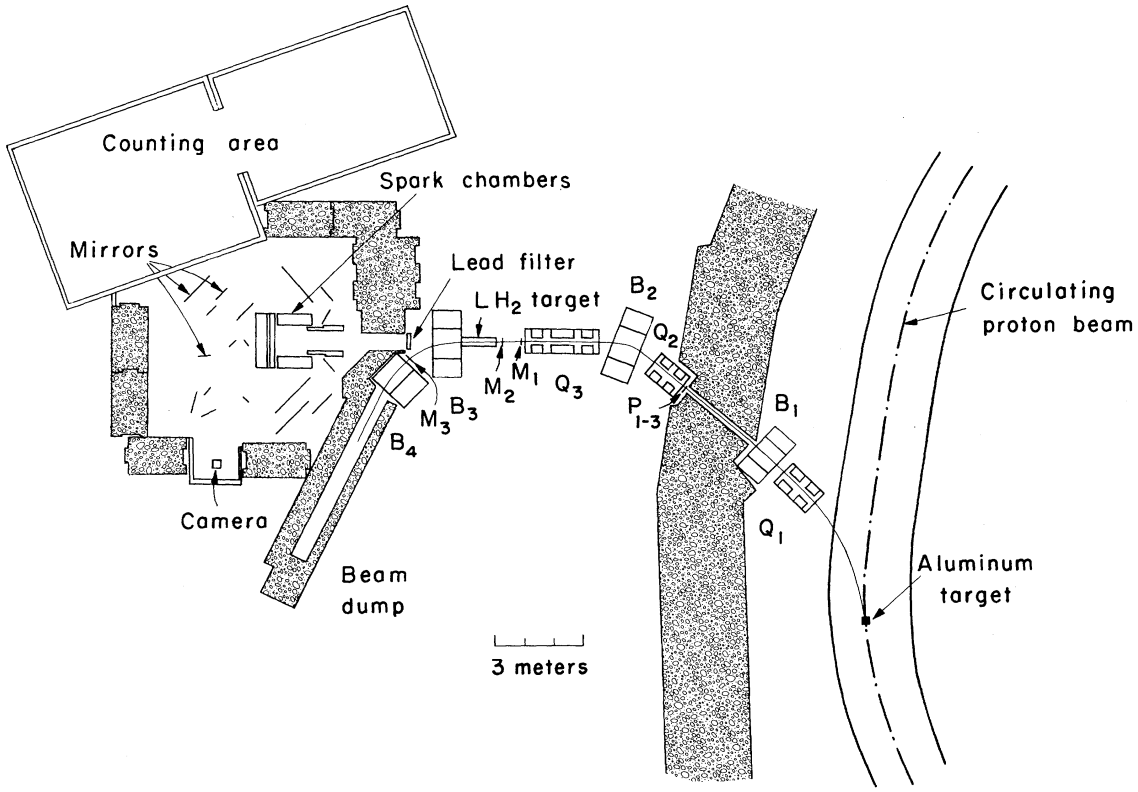

FIG. 1. Plan view of the experiment.

The basic objectives of the experimental method were (1) to make the single-γ-ray detection efficiency high enough so that the efficiency to detect all four γ rays from a $K_L^0 \to 2\pi^0$ decay was not a sensitive function of the chamber parameters and thus most (95%) of the background events ($K_L^0 \to 3\pi^0 \to 6$ γ rays) were eliminated simply by the observation of five or more showers; (2) to use an unrestrictive condition for the spark-chamber trigger so as to detect the $2\pi^0$ and $3\pi^0$ decays with comparable efficiencies and little kinematic bias, allowing the use of the $3\pi^0$ decays for normalization; (3) to analyze all of the four-shower events for the presence of a $2\pi^0$ intermediate state using information on γ-ray directions and energies provided by the shower directions and spark counts; (4) to determine the number of $2\pi^0$ events in the four-shower sample by adjusting the relative amounts of Monte Carlo generated $2\pi^0$ and $3\pi^0$ four-shower events until the best fit was made to the distributions obtained from the data.

Calibrations of the system required by the analysis and Monte Carlo programs were obtained by direct measurements. The pointing accuracy and spark-count energy resolution of the γ-ray showers were obtained from the following auxiliary studies:

(1) Study of $K_L^0 \to \pi^+\pi^-\pi^0$, $\pi^0 \to 2\gamma$. Observation of the charged pion tracks and knowledge about the K_L^0 momentum enabled calculation of γ-ray energies and directions. Thus the pointing errors, spark counts, and shower patterns in the chambers for γ rays of known energy up to 200 MeV were determined.

(2) Study of $\pi^- p \to \eta^0 n$, $\eta^0 \to 2\gamma$. The data for this study were provided by a separate experiment[4] utilizing the same spark chamber array but with the addition of neutron time-of-flight counters placed outside and a hydrogen target placed inside the array. Calibration of the spark-count technique for γ rays of known energy in the range 175 to 450 MeV was thereby obtained.

(3) Study of γ rays from a small (1.3-cm cube) aluminum target placed in a pion beam at the center of the decay volume. This study provided shower pointing accuracy information for γ-ray energies to more than 500 MeV as deduced from spark counting.

The γ-ray calibration data were put directly into the Monte Carlo program in the form of a library of 751 case histories of shower development for γ rays of known energy. The response of the spark chambers to a particular γ ray was determined by selecting the shower case history

(together with its spark count and pointing error) having the closest energy. The Monte Carlo program thus did not rely on any adjustable shower parameters, and the agreement of its prediction with the $K_L^0 \to 2\pi^0, 3\pi^0$ data provided an independent test of the program. Independent tests were also provided by the following:

(1) Additional data taken with a beryllium regenerator placed in the decay volume were used to check the analysis and Monte Carlo programs. The regenerator data provided a supply of $2\pi^0$ events similar to $K_L^0 \to 2\pi^0$ decays. To the extent that the beryllium regeneration amplitudes are known, the data provided a check of the $2\pi^0$ analysis efficiency predicted by the Monte Carlo program. Data with thin slabs of beryllium in the decay volume were also used to determine the subtraction required to account for the small background from air interactions.

(2) The over-all rate from all charged K_L^0 decays was used, together with a Monte Carlo calculation of the charged trigger efficiency, to check the more difficult calculation of the $3\pi^0$ trigger efficiency.

(3) The beam monitor rate and measured beam composition together with known K production and absorption cross sections, lifetime and branching ratios, were used to check the calculated $3\pi^0$ trigger efficiency.

III. BEAM AND APPARATUS

A. Beam design and K^0 production

The pion beam at the liquid hydrogen target was designed to have its maximum momentum just below the $K^0\Sigma^0$ threshold. Its minimum momentum was high enough to prevent excessive spread of the forward K^0 momentum in the $\pi^- p \to K^0\Lambda^0$ production reaction.

Helium bags were used between the Bevatron thin window and beam monitor counter M_1. A second monitor, M_2, was placed immediately ahead of the hydrogen target, and a third, M_3, was placed after the target and the first sweeping magnet to veto noninteracting particles.

The pion momentum spectrum is shown in Fig. 2. It was determined with 1% resolution by using counter hodoscopes to measure pion deflections in traversing the sweeping magnet B_3. A typical 800-msec Bevatron pulse of 5×10^{11} protons at 5.6 GeV produced 13×10^6 beam particles incident on the hydrogen target. By studying the relative counting rate of a high pressure Čerenkov counter as a function of pressure, the beam composition was found to be 67% pions, 12% muons, and 21% electrons.

Forward-going γ-rays, K_L^0's, and neutrons produced in the target entered a γ-ray filter placed 1.8 m from the downstream end of the target. The filter consisted of four sheets of lead, in succession 2.54, 3.18, 2.54, and 1.90 cm thick, each followed by a scintillation counter (L_1 through L_4). The lead thickness was optimized to remove photons and retain K_L^0's.

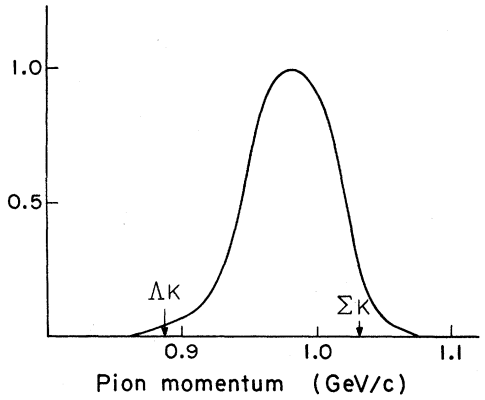

FIG. 2. Measured momentum distribution of the π^- beam at the hydrogen target. Thresholds for Λ^0 and Σ^0 production are shown. The vertical scale is linear.

Following the filter, the remaining K_L^0's and neutrons passed through a 0.6-m by 0.6-m channel in a 1.5-m-thick steel collimator, through a four-sided shower counter tunnel surrounding the flight path, and then entered the 1-m cubic decay volume that started 5.1 m from the end of the hydrogen target.

The K_L^0 momentum distribution was calculated by Monte Carlo techniques using the known cross sections for K^0 production.[5] The effect of ionization energy loss by the pions in the liquid hydrogen was taken into account, but the momentum variation of the absorption of pions in the hydrogen and of K_L^0's in both the hydrogen and the lead filter had a negligible effect on the shape of the momentum spectrum of the K_L^0 beam. The variation in survival against decay for K_L^0's of different momentum was included in calculating the momentum distribution of the K_L^0 beam at the entrance to the spark chamber array. This distribution is shown in Fig. 3.

A typical Bevatron pulse resulted in about 40 K_L^0's and 700 neutrons entering the decay volume. The small neutron background caused no difficulty in the performance and analysis of the experiment; only a small fraction interact in the decay volume and an even smaller fraction trigger the chambers. Operation with the hydrogen target empty gave an observed rate of K_L^0 decays less than 2% of the full rate, consistent with that expected from K^0 production in the target end windows and the monitor counter scintillator.

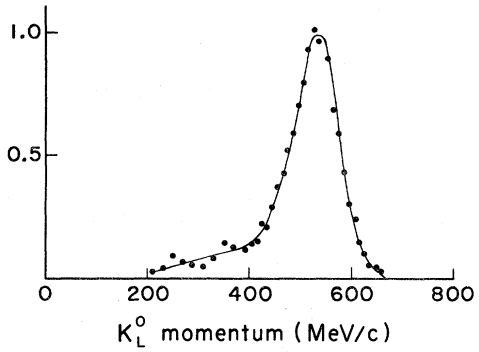

FIG. 3. Calculated momentum distribution of the K_L^0 beam at the entrance to the spark chamber array. The points are the results of the calculation. The vertical scale is linear.

B. γ-ray detectors

1. General design

The arrangement of the γ-ray detectors is shown in Figs. 4 and 5. The 1-m^3 decay volume was surrounded on five sides by lead-plate spark chambers about 7 radiation lengths thick. The upstream side was left open for the entering K_L^0 mesons. The decay volume was further enclosed by placing, at the entrance to the spark chamber array, a γ-ray shower counter in the shape of a four-sided tunnel. The total solid angle subtended by the γ-ray detection assembly was 98% of 4π in the K_L^0 barycentric system.

The use of a large decay volume required by the low intensity of the nearly monoenergetic K_L^0 beam resulted in generally good spatial separation of the showers permitting unambiguous identification of the shower multiplicities of nearly all events.

2. The spark chambers

The first element in each of the five spark chambers was a four-gap aluminum module, 0.06 radiation lengths thick, used to identify entering charged particles. The rest of the modules contained plates of 0.8-mm lead laminated between two 0.4-mm aluminum sheets to convert the γ rays and to develop the shower. These six-gap modules were 5.9 cm thick and contained 0.915 radiation lengths of material. The downstream chamber was 198 cm by 198 cm and consisted of an aluminum module followed by eight lead modules. The four side chambers were 122 cm by 152 cm and consisted of one aluminum module followed by seven lead modules.

3. Counters

The shower counter configuration is shown in Figs. 4 and 5. The entrance tunnel to the spark-chamber array contained independent shower counters in each of its four sides ($T_1 - T_4$). Each counter was 122 cm long in the beam direction and 91 cm wide. The counters were 5.7 radiation lengths thick except for the upstream half which was 8.5 radiation lengths thick. The tunnel extended 15 cm into the region enclosed by the spark chambers. The counters were constructed by interleaving sheets of 0.8-mm lead and 3-mm Lucite preceded by a single 6-mm sheet of scintillator to detect

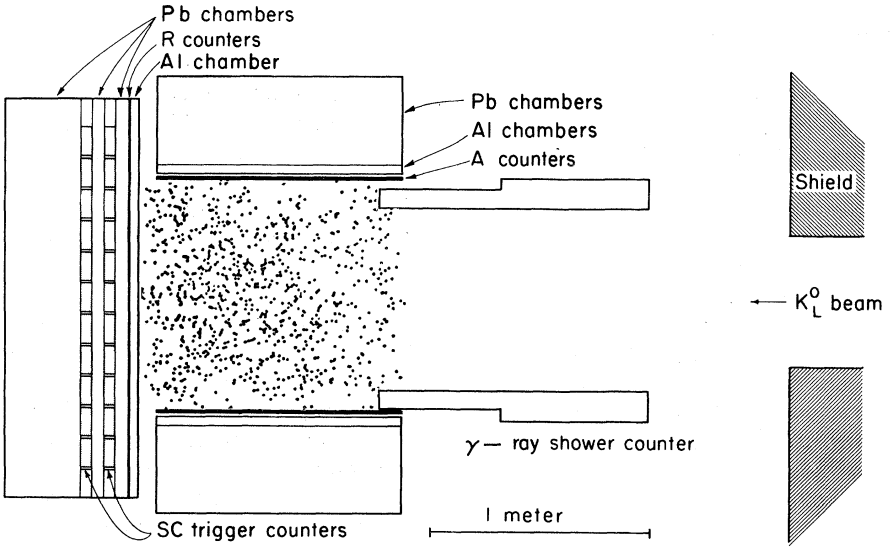

FIG. 4. Vertical section through γ-ray detection assembly. Vertices of four-shower events having no counts in the tunnel shower counter are projected on this plane. Vertices of $2\pi^0$ events have a similar distribution. The volume enclosed by the spark chambers is a one-meter cube. The fiducial-volume boundaries are 5 cm from the chambers.

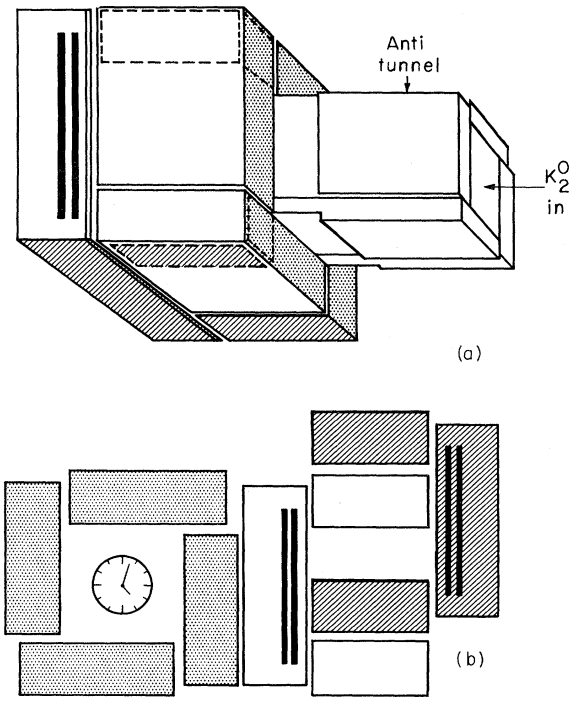

FIG. 5 (a) Perspective drawing of spark chamber array and tunnel shower counter. (b) Layout on film of views of spark chamber array. The shading indicates the correspondence between the views in the two drawings.

slow charged particles. The upstream edge of each counter was viewed by six 58AVP phototubes whose outputs were added to form a single signal for each of the four counters.

Showers from neutral decays were detected by two banks of trigger counters placed after the first and second lead modules in the downstream spark chambers. Each bank consisted of a vertical stack of 11 horizontal counters ($SC_1 - SC_{11}$) which were 1.55 m long and 11 cm high. Each counter consisted of a 6-mm scintillator and a 38-mm slab of Lucite as a Čerenkov counter. The scintillator provided fast timing and the Čerenkov was used to prevent counts from np recoils. The two Čerenkov radiators at the same height in the two banks were combined optically at a 58AVP phototube, while the signals from the corresponding scintillators were added passively at the bases.

Placing trigger counters in the downstream rather than the side chambers brought two disadvantages: The spurious trigger rate was high (only 6% of the pictures showed K_L^0 decays), and the sensitivity to $K_L^0 \to 2\gamma$ was too low to use that as a monitor. The advantages were a relatively high trigger efficiency for both $2\pi^0$ and $3\pi^0$ decays (~20%) and the ability to use the same counters for charged decay calibration runs (the charged particles go predominantly forward).

In order to veto charged particles, twelve 6-mm-thick scintillators (A_1 through A_{12}, three covering each of the four side walls of the decay volume) were mounted inside the four aluminum side chambers. Six scintillators ($R_1 - R_6$) each 6 mm thick, 33 cm wide, and 198 cm long were placed one above the other between the downstream aluminum module and the first lead module to form a wall that also served to veto cosmic rays.

4. *Optical system*

Two orthogonal views of each spark chamber were combined into one frame by a system of 46 front-surfaced mirrors. The ten views were arranged on the film in three groups. The correspondence between the views on the film and views in real space is shown in Fig. 5. Within each view the geometrical relationship between the chambers was nearly the same on the film as it was in real space. This arrangement facilitated the recognition of showers passing through more than one chamber and made it possible to count accurately the number of showers present in an event at the scanning stage of the analysis. In addition, some accidental tracks could be eliminated because it was obvious they did not come from the vertex formed by the other showers in the event.

C. Electronics and counter logic

The electronic signature corresponding to the possible production of a K^0 was taken to be $M_1 M_2 \bar{M}_3 \bar{L}_1 \bar{L}_2 \bar{L}_3 \bar{L}_4 = M$. The data were usually taken at pion beam rates of 10–15 MHz, using 100-MHz electronics. Special precautions were taken where necessary for stable operation. dc coupled veto circuits and amplifiers were used in high-rate channels, and Zener diodes and booster current supplies were used in the last stages of busy phototubes. Deadtime losses in the $M_1 M_2$ circuit were about 20%, but this matched the deadtime in the spark chamber trigger logic so that the monitor always tracked the number of K decays on film to within a few percent. This monitor was used to normalize the $2\pi^0$ and $3\pi^0$ data with the charged decay and regenerator data, but was not needed for the measurement of the $2\pi^0/3\pi^0$ branching ratio.

The signature for a K_L^0 decay into a neutral final state was taken to be (1) fulfillment of the K^0 production requirement (M), (2) no response from the A scintillation counters lining the side walls of the spark chambers, (3) no response from the R scintillation counters embedded in the downstream chamber after the first aluminum module, and (4) response from at least two of the SC scintillator-Čerenkov trigger units separated by a minimum distance of two counters. This separation reduced the spurious trigger rate from single particles crossing from one SC unit to an adjacent one and from groups of γ rays coming from the lead filter. Allowing any two such units to provide the trigger produced one that was free of major kinematical bias.

Time-coincident signals from the tunnel shower counter turned on a data light which was recorded on the spark chamber film. In addition, a signal formed from the sum of the tunnel counter outputs and delayed by one Bevatron rf cycle provided information on the accidental rate. In a similar fashion, counts in the SC trigger units lit data lights mounted on the side of the downstream chamber directly over the ends of the corresponding counters. The trigger lights provided identification of low-energy γ-ray showers which fired a trigger counter but produced only one or two sparks in the chamber and were also used to discriminate against accidental tracks in the downstream chamber. Events having showers passing through three or more separated SC units provided a continuous monitor of the SC efficiency.

The signature of a K_L^0 decay into a charged final state was taken to be (1) fulfillment of the K^0 production requirement (M), (2) no response from the A scintillation counters, (3) no response from the top or bottom R counters, (4) response from two or more of the four inner R counters, and (5) response from two or more of the trigger scintillators separated by a minimum distance of one trigger unit. The Čerenkov requirement was removed for this mode since not all of the decay pions and muons have a sufficient velocity to be detected with a high and reliable efficiency. Because conversion from neutral to charged decay was simple, the type of data acquisition was alternated frequently throughout the run.

The S, C, A, R, and T counters were timed relative to one another using either γ rays from $\pi^- p \to \pi^0 n$ or cosmic rays. Timing relative to M was done by maximizing the yield of K_L^0 events seen in the spark chambers. All timing curves were required to have flat tops to ensure a high and stable efficiency. The circuits combining the SC pairs had unavoidably broad resolution times (20 to 40 nsec) due to differences in the various particle and light collection paths; nevertheless, the accidental trigger rate was less than 25% at maximum beam intensities. These triggers resulted mainly from interactions in the lead filter which gave two or more time-coincident γ rays with degraded energy.

When the signature for the production and decay of a K_L^0 was met the electronics were gated off and the spark chambers triggered. The rate was one to two pictures/pulse for the neutral signature and five to six pictures/pulse for the charged signature. The electronics block diagram is shown in Fig. 6.

D. Chamber operation and performance

Stable operation of the chambers was ensured by an automatic monitor system which successively examined the pulses on each double gap and sounded an alarm when the delay time, peak height, or fall time were not within certain preset limits.

A systematic error can arise if accidental showers are present in the chambers, since this would result in an uncompensated loss of four-shower $2\pi^0$ events. To study such possibilities, runs were made in which the chambers were pulsed each time a preset number of beam particles was counted. A preset delay, long compared with the average time between beam particles, made the pulses essentially random but weighted with respect to the average beam intensity in the same way K_L^0 events would be weighted. Runs were also made with a 91-cm-high by 89-cm-wide by 12.3-cm-thick beryllium slab placed in the decay volume 86 cm from the downstream chamber. The results of this study are shown in Table I.

The number of spurious sparks was small, partially because of the shaped chamber pulse.[6] This allowed a two-adjacent-spark minimum for identification of a shower. The adoption of the two-spark minimum was not necessary to achieve a high efficiency for detecting $2\pi^0$ events (regenerator studies showed that 98% of the showers from $2\pi^0$ events showed five or more sparks), but was useful in detecting low-energy γ's from $3\pi^0$ events and hence improved the background rejection of the experiment. With the use of a two-spark minimum, Table I shows that about 9% of the $2\pi^0$ events were lost because of the appearance of either an accidental shower or an accidental tunnel counter signal. Tracks due to entering charged particles or np recoils in the downstream chamber occurred in only a few percent of the frames, were easily distinguished from showering tracks, and so presented no problem to the identification of K_L^0 decays.

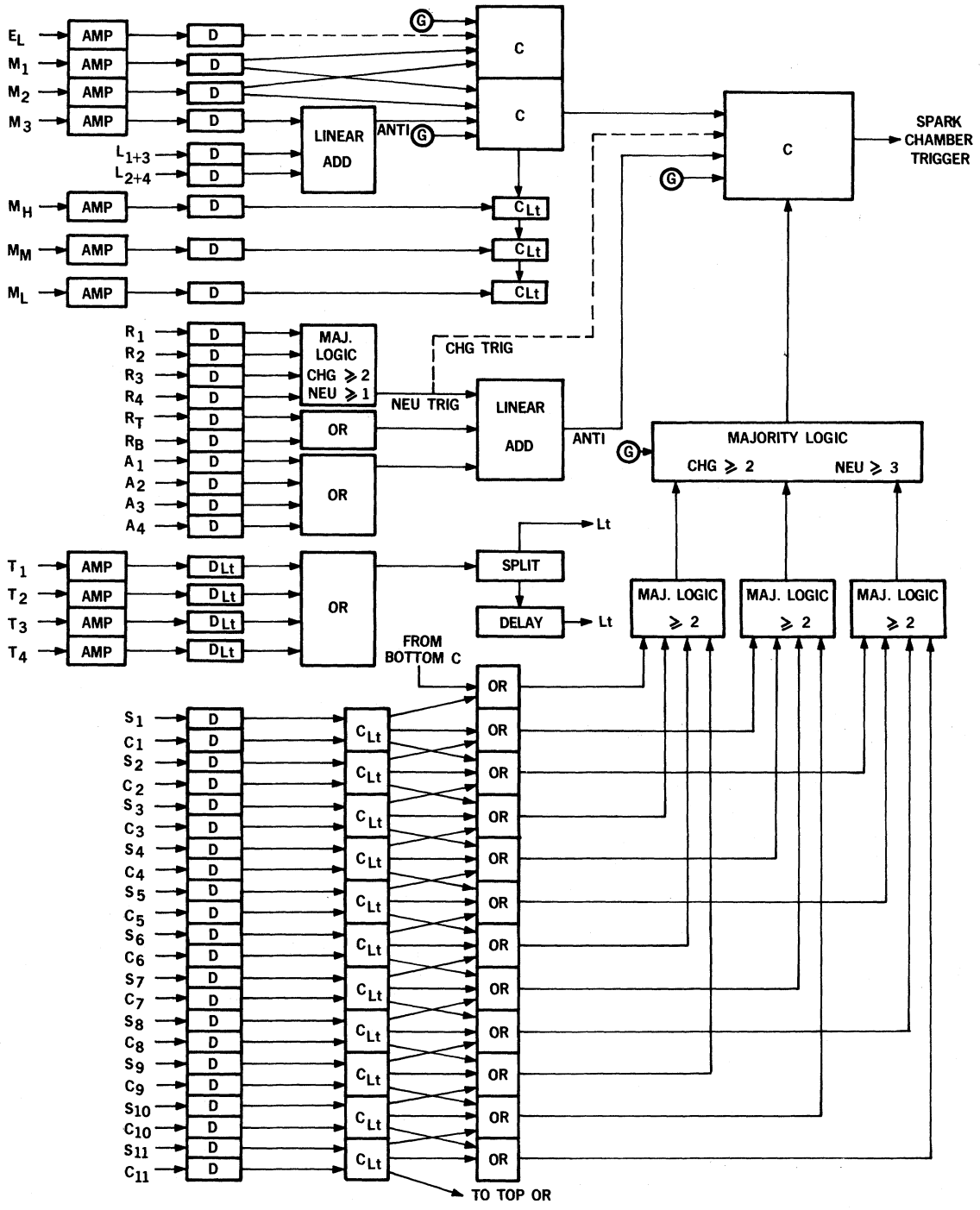

FIG. 6. Block diagram of fast electronics. Discriminators are denoted by the letter D, coincidence circuits by the letter C, and Lt indicates a signal which is displayed as a data light and photographed with each event.

TABLE I. Results of scan of random-pulsing data.

	Air		Be
Beam particles $\times 10^{-6}$/Bevatron pulse	13.3	26.2	13.3
Number of frames	1763	419	1668
Average number of isolated sparks/frame	1.5	2.5	•••
		% of frames	
Tunnel counter signals	4.2± 0.4	8.8± 1.4	3.7± 0.5
2-spark showers in lead chambers	1.6± 0.3	2.9± 0.8	6.6± 0.6
≥ 3-spark showers in lead chambers	1.4± 0.3	4.8± 1.1	4.5± 0.5
Entering charged particles	2.4± 0.4	6.9± 1.3	2.0± 0.3
np recoils	0.1	0.7	0.7
SC counts	0.1	0.1	0.2

IV. ANALYSIS OF EVENTS

A. Scanning

464 000 (2.557×10^{12} $M_1 M_2$ counts) spark-chamber pictures were taken using the neutral trigger described in Sec. III C. This film was scanned to provide a count of the total number of neutral decays of the K_L^0 observed during the run and to select a subset of events which could possibly be $K_L^0 \to 2\pi^0$ decays.

Neutral decay events were required only to have three or more showers, each having three or more sparks, forming a vertex which could conceivably be in the decay volume. This scanning criterion was also satisfied by background events in which a neutron interacted in the air to produce a neutral final state which included two π^0's and by events in which a K_S^0 was regenerated in the air and which then decayed into two π^0's. However, data taken with beryllium and carbon slabs placed in the decay volume showed that less than 1% of the events were due to interactions in the air. From the observed pointing errors and angular distributions, it was expected that less than one event was due to unrelated γ rays pointing to a vertex within the decay volume. The scan of the 2000 frames taken with a random trigger (discussed in Sec. III D) showed no events in which there were even two showers with three or more sparks present in the chambers. Consequently we are confident that the above scanning criterion provided nearly certain identification of K_L^0 neutral decays.

Each roll of film was scanned twice. About 20% of the film was scanned a third time by physicists. This check scan showed the efficiency for at least one of the two scanners to record a K_L^0 neutral decay was greater than 99%. Over 30 000 such decays were found.

The precise determination of the number of showers in an event was a more difficult problem. Since most of the $3\pi^0$ decays were separated from $2\pi^0$ decays simply by the detection of five or more showers, it was very important that this process be as free from error as possible. Each event on the combined list from the first two scans was examined by a physicist to determine the number of showers present. The four-shower events with no tunnel shower counts were candidates for $2\pi^0$ decays, and were divided into certain and doubtful classes. In the doubtful cases there was usually a fifth shower present which probably came from the decay point but which could possibly have been produced by bremsstrahlung in one of the other showers. The distinction between these two classes of events was carried through the entire analysis. No $2\pi^0$ events were found in the doubtful class so it could be dropped with no loss of selection efficiency. The selection efficiency was estimated to be (98 ± 2)% by having another physicist perform a second selection.

B. Measurements

1. Direction measurements

Shower directions were determined by measuring all the sparks in the shower up to the point where the track first noticeably deviated from a straight line, usually after three to five sparks. A straight line was fitted through the measured points of each shower, giving equal weight to each spark. Showers with obviously serious pointing errors were flagged; their conversion-point location was used but their direction was not. Examples are two-spark showers, and showers that start in a spark-chamber frame or other insensitive region.

2. Spark-count measurements

The energy of the shower was estimated by measuring the total apparent path lengths of the electrons in the lead plates. The sum of these lengths

was expressed as the number of equivalent sparks which would be visible for an electron traveling normally to the plates. Isolated sparks were counted and added to the equivalent spark total. Energy lost by the shower in traversing the trigger counters in the downstream chamber was also taken into account. The uncertainty in range for showers which did not pass all the way through a counter was reduced by using the information provided by the data lights which indicated whether or not the trigger counter had been fired. Showers with large probable spark-count errors were flagged. Examples are showers that run out the back of a chamber while still well developed and showers that cross insensitive areas such as chamber frames.

3. *Fiducial volume*

In order to normalize the $2\pi^0$ rate to the $3\pi^0$ rate it was necessary to apply a fiducial-volume cut to both types of events. The boundaries of the fiducial volume were taken to be 5 cm away from any solid material to prevent possible contamination of the data by $2\pi^0$ decays of K_S^0 mesons regenerated in the tunnel shower counter or in the spark-chamber plates. The 5-cm margin was safely greater than the usual uncertainty of 1 to 2 cm in the location of the decay point for events close to the chambers. The fiducial volume was a rectangular prism with dimensions 102 cm by 102 cm perpendicular to the beam and 96 cm along the beam.

C. Kinematic fitting of four-shower events

The locations of the source of the K_L^0 and the beginning points of the showers were all known with relatively high precision. To determine the location of the decay point (and thus the γ ray and K_L^0 direction) a search operation was performed using the shower directions and spark counts as fixed input data. For an assumed decay point, the hypothesis that the four γ rays came from a $2\pi^0$ state determined the γ-ray energies up to a sixfold ambiguity. Assuming nothing about the parent mass or momentum, the kinematic constraints corresponding to a $2\pi^0$ intermediate state could be expressed by four equations: two conservation of transverse momentum equations and the two invariant-mass equations

$$\begin{aligned} 2P_1P_2(1-\cos\theta_{12}) &= m_\pi^2 \,, \\ 2P_3P_4(1-\cos\theta_{34}) &= m_\pi^2 \,, \end{aligned} \tag{1}$$

where θ is the angle between each pair of γ rays and P_1–P_4 are their momenta. There are three sets of these equations corresponding to the three possible pairings of the γ rays, and for each set there are two possible analytical solutions.[7]

The first step in the search procedure was to estimate the location of the decay point directly from the shower directions, using an analytical calculation to find the common point having the minimum weighted distance to the shower lines. The weights depended upon the shower pointing errors determined from their spark counts. The six sets of γ-ray energies were calculated using the directions of the particles deduced from this starting point. For the sets (usually two to four) which gave four positive energies, the location of the decay point was varied (new γ-ray energies were calculated at each point) until the best fit to the shower directions and spark counts was found.

The goodness-of-fit measure was defined as

$$\chi^2 = \frac{4}{n}\sum_{i=1}^{n}\left(\frac{E_{\gamma,\,\mathrm{kin}} - E_{\gamma,\,\mathrm{spk\ cnt}}}{\sigma_E(E_{\gamma,\,\mathrm{kin}})}\right)^2 + \frac{4}{m}\sum_{i=1}^{m}\chi_A^2\left(\frac{\delta\theta}{\sigma_A}\right) . \tag{2}$$

The sums are taken over all unflagged showers ($1 \leq n \leq 4$; $2 \leq m \leq 4$; $\langle n\rangle = 3.7$, $\langle m\rangle = 3.2$). The expected errors, σ_E and σ_A, are determined from the kinematic energies of the γ rays using distributions of spark-count errors and pointing errors obtained from direct calibrations discussed in Sec. IV D. Because the calibration distribution for angular errors was non-Gaussian in the variable

$$\frac{\delta\theta}{\sigma_A} = \frac{\theta_{\mathrm{shower}} - \theta_{\mathrm{gamma}}}{\langle\delta\theta\rangle_{\mathrm{rms}}} ,$$

where $\langle\delta\theta\rangle_{\mathrm{rms}}$ was a function of $E_{\gamma,\,\mathrm{kin}}$, we determined χ_A^2 for each shower as a nonlinear function of $\delta\theta/\sigma_A$ in such a way that χ_A^2 was normally distributed for the calibration data. Also, the spark-count flag (indicating lost energy) was removed when E_{kin} was less than E_{spark}.

Since it was possible that the correct pairing did not have a physical solution at the starting point, six other points were also used as starting points in the search. The six alternate points were located along each of the coordinate axes at distances of $\pm\sigma$ from the original point. After the ≤ 42 search operations (seven initial points times three pairings times ≤ 2 solutions per pairing) had been carried out, the point with the lowest value for χ^2 was chosen to be the decay point. The γ-ray energies given by the solution corresponding to this pairing and decay point were used to calculate the mass and momentum of the parent particle.

If four positive energies were found at an initial

point for a given pairing and solution, then four positive energies could generally be found for most of the other initial points. The search program was almost always able to find the minimum point starting from any of these initial points. Analysis of Monte Carlo-generated $2\pi^0$ events showed that the efficiency of the search program to find a solution with $\chi^2 < 12$, a momentum between 420 MeV/c and 700 MeV/c, and a mass greater than 450 MeV was 67%.

D. Calibrations of the spark chambers

1. $K_L^0 \to \pi^+\pi^-\pi^0$

Calibration of the shower pointing accuracy and spark counts for γ rays of known energy in the range 0 to 200 MeV were determined from the analysis of $K_L^0 \to \pi^+\pi^-\pi^0$ events. Out of 170 000 (2.01×10^{11} $M_1 M_2$ counts) spark-chamber pictures taken under the charged signature described in Sec. III C, there were about 4000 leptonic and 1000 $K_L^0 \to \pi^+\pi^-\pi^0$ decays. The latter were identified by the presence of two entering, nonshowering tracks in the downstream chamber forming a vertex which could possibly be in the decay volume, together with the presence of at least one γ ray possibly pointing to this vertex. Of these events, 1.5% showed three γ rays, 67% showed two γ rays, 5.5% showed two γ rays and a tunnel count, 17% showed one γ ray, and 9% showed one γ ray and a tunnel count.

Only those events without tunnel counts and in which two γ rays converted in the sensitive volume of the chambers were used for calibration purposes. The vertex formed by the two charged pions was taken to be the decay point and the energies of the decay particles were calculated using the three conservation-of-momentum equations and the invariant-mass equation for the π^0. The γ-ray energies and directions, determined without using any information from the showers except the locations of their conversion points, were then compared to the observed shower directions and spark counts. A scatter plot of spark counts versus kinematically determined γ-ray energies is shown in Fig. 7. A similar scatter plot of shower pointing errors versus γ-ray energies is shown in Fig. 8.

The sensitivity of the calibration to pointing

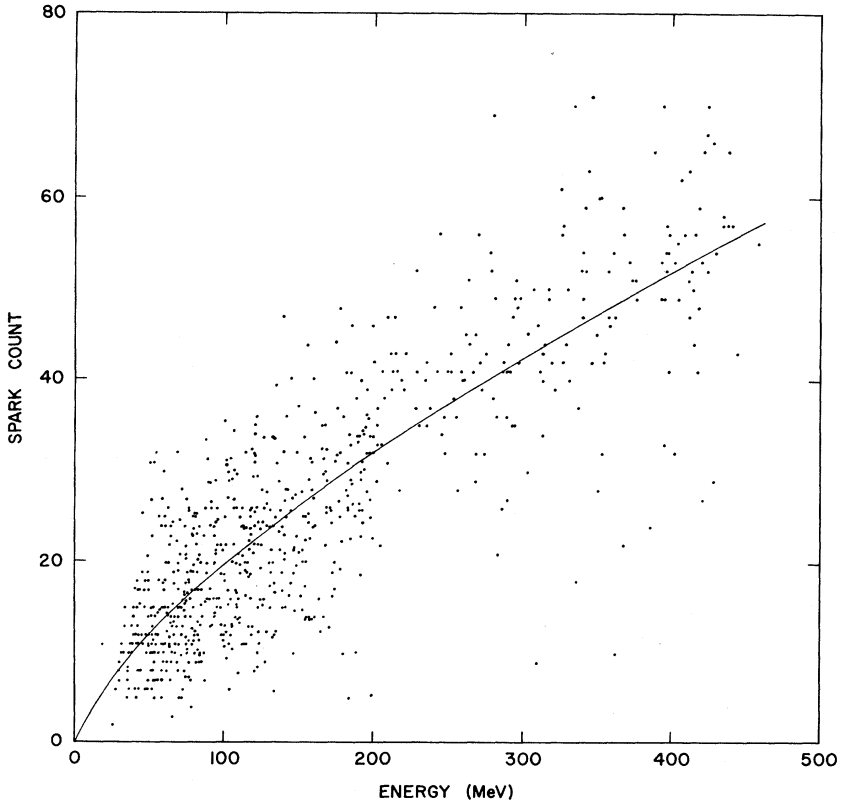

FIG. 7. Scatter plot of spark count vs γ-ray energy for combined $K_L^0 \to \pi^+\pi^-\pi^0$ and $\eta \to 2\gamma$ data. The curve shown is the least-squares fit to the data of a function of the form AE^B, where E is the energy of the γ ray in MeV. The values of A and B were determined to be 0.777 and 0.701, respectively.

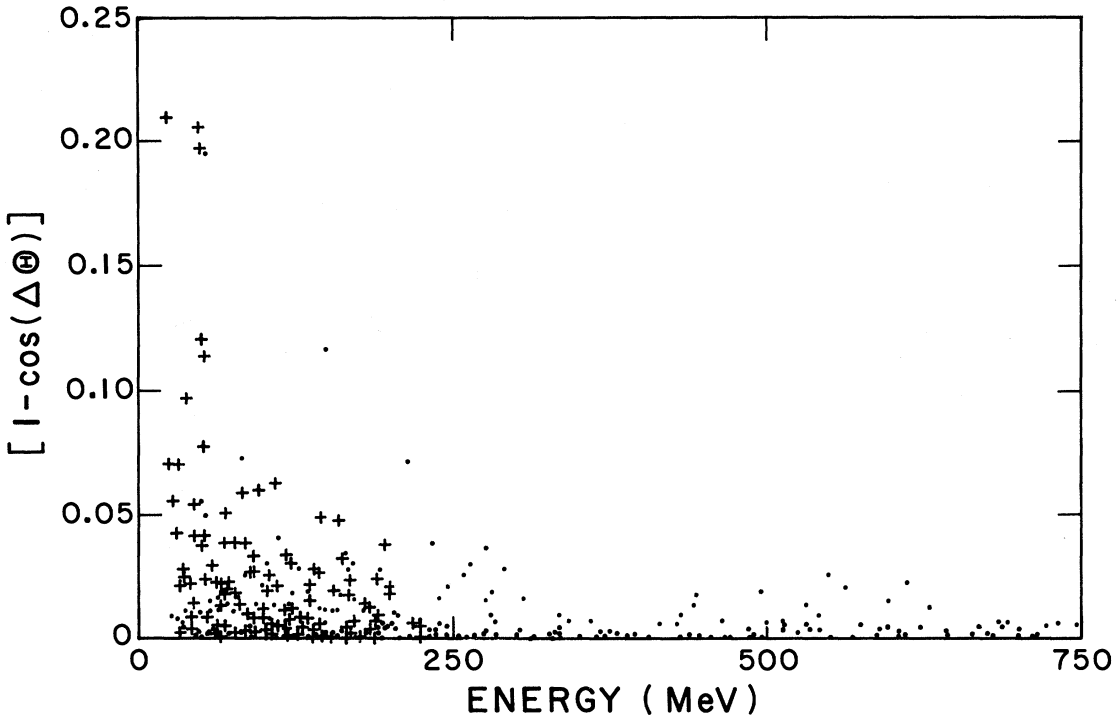

FIG. 8. Scatter plot of shower pointing error vs γ-ray energy. The χ's are from $K_L^0 \to \pi^+\pi^-\pi^0$ data; dots are aluminum target data.

errors in the charged pion tracks was found by varying the charged pion directions by an amount comparable to their errors. Events in which either the γ-ray energies or their pointing errors changed significantly were infrequent and were not used in the calibration data.

2. $\pi^- p \to \eta^0 n, \eta^0 \to 2\gamma$

Following the K_L^0 run, the spark chambers were used to study neutral decay modes of the η.[4] A 7.5-cm diameter by 20-cm-long liquid hydrogen target was placed in the center of the decay volume and a 716 ±10-MeV/c π^- beam was brought in. The K_L^0 counter system was replaced with anticoincidence counters surrounding all but the upstream face of the hydrogen target and a ring of neutron time-of-flight counters placed at the Jacobian peak angle. Those two-shower events having a neutron time-of-flight corresponding to an ηn final state contained less than 2% background and were analyzed with a 3C fit that constrained the $\gamma\gamma$ mass to equal the η mass. The energy of the showers ranged from 175 to 450 MeV and was known with an average error of ±10 MeV. As was the case for $K_L^0 \to \pi^+\pi^-\pi^0$ events none of the information from the shower itself was used other than the location of the conversion point and the fact that the shower had two or more sparks; consequently no significant bias is expected in this population of showers. The spark counts versus γ-ray energies for the η data are plotted along with $K_L^0 \to \pi^+\pi^-\pi^0$ data in Fig. 7. The two types of data agreed well in the overlap region between 175 and 200 MeV.

3. *Aluminum-target data*

While the η run gave high-energy γ rays of well-known energy permitting the study of shower structures and spark counts, the size of the hydrogen target did not permit an adequate determination of shower pointing errors. To obtain a well-localized source of γ rays the hydrogen target was replaced by a 1.3-cm cube of aluminum. The spark chambers were triggered on beam pions which interacted in the aluminum target. The energies of the γ rays could not be determined kinematically, so instead were deduced from the shower spark counts. The pointing errors of showers versus the γ-ray energies are plotted along with the corresponding data from $K_L^0 \to \pi^+\pi^-\pi^0$ decays in Fig. 8. The two types of data agreed well in the overlap region from 0 to 200 MeV.

V. ANALYSIS OF EVENT DISTRIBUTIONS

A. General method

The calculation of the number of $2\pi^0$ events in the four-shower sample required knowledge of the behavior of both $2\pi^0$ and $3\pi^0$ events under the analysis program. A Monte Carlo computer program was written to simulate the appearance of both types of events in the experimental apparatus. Sets of $2\pi^0$ and $3\pi^0$ four-shower events were generated and analyzed in the same way as the data. The distribution for the four-shower data was then fitted by a sum of Monte Carlo $2\pi^0$ and $3\pi^0$ distributions using a maximum-likelihood technique. The calculation of the relative rates $(K_L^0 \to 2\pi^0)/(K_L^0 \to 3\pi^0)$ from the observed numbers of $2\pi^0$ and $3\pi^0$ events, n_2 and n_3, required a further use of the Monte Carlo program to find the proportionality constant, R, relating them:

$$R = \frac{K_L^0 \to 2\pi^0 \text{ rate}}{K_L^0 \to 3\pi^0 \text{ rate}} = \left(\frac{D_3 t_3 s_3 f_3}{D_2 t_2 s_2 f_2 a_2}\right) \frac{n_2}{n_3}, \qquad (3)$$

where

D_3 (D_2) = probability that none of the 3 (2) pions undergo a Dalitz decay which would veto the event (e^+e^- pairs almost always trigger veto counters),

t_3 (t_2) = probability of a 3- (2-) pion decay triggering the spark chambers,

s_3 (s_2) = probability of a triggering 3- (2-) pion decay giving ≥ 3 (4) visible showers in the chamber,

f_3 (f_2) = probability of such an event having its vertex reconstructed within the fiducial volume,

a_2 = probability of a 2-pion, 4-shower event not having an accidental shower or tunnel count (3-pion decays are not rejected because of such accidentals).

The ratio of trigger efficiencies, t_3/t_2, proved to be quite insensitive to the details of the Monte Carlo program, to refinements added during its development, and to variations deliberately introduced to check its sensitivity to experimental error. The efficiency s_3 was essentially unity (see Fig. 9). The efficiency s_2 was close enough to unity (0.67) to be reliably calculated.

B. Monte Carlo program

1. *Generation of $K_L^0 \to 2\pi^0, 3\pi^0$ decays*

K_L^0 mesons with the known momentum distribution for the experiment were generated and allowed to decay in a region which extended beyond the fiducial volume 7.5 cm downstream and 15 cm upstream and whose lateral extent was determined by the 86-cm by 86-cm entrance aperture formed by the tunnel shower counter. The $3\pi^0$ decays were uniformly distributed over three-body Lorentz-invariant phase space with the plane containing the three pion momentum vectors randomly oriented in space. The distribution of $3\pi^0$ decays on a Dalitz plot has been directly measured with this apparatus, using a large (>5000) sample of six-shower events.[8] Within errors, it is completely uniform, with a radial distribution

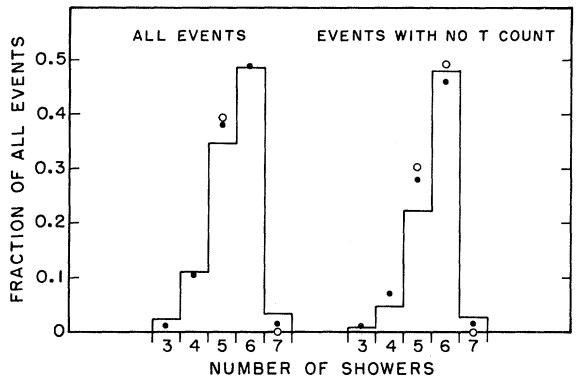

FIG. 9. Shower multiplicities in the spark chambers for K_L^0 decays reconstructed to have occurred in the fiducial volume. The solid circles are the Monte Carlo predictions for $K_L^0 \to 3\pi^0$ events corrected for the presence of accidental showers. The open circles are the $K_L^0 \to 3\pi^0$ predictions not corrected for accidental showers. If the two symbols overlap only the solid circle is shown. There is only one over-all normalization (to all events) and so knowledge of the T efficiency is required here (though not for the final experimental result).

$$\rho(r) = 1 + (0.03 \pm 0.02) r^2 + (0.01 \pm 0.02) r^4, \qquad (4)$$

where r is the fractional distance to the boundary. A uniform distribution has also been found by Heusse *et al.*[9] Regenerated coherent and incoherent $K_S \to 2\pi^0$ events were generated by the Monte Carlo program with the appropriate spatial and angular distributions.

2. *Shower library*

Monte Carlo programs involving γ-ray showers are particularly prone to error since it is difficult to construct a model which adequately describes the complexity of shower development. Adjusting parameters may make an inaccurate model fit some distributions but still give incorrect efficiencies. To avoid this we used the calibration data discussed in Sec. IV D directly to make a library of 751 shower case histories. Each case history was labeled by its energy as determined from the $K_L^0 \to \pi^+\pi^-\pi^0$, $\pi^0 \to 2\gamma$, or $\eta \to 2\gamma$ kinematics and contained a one-dimensional representation of the shower pattern (except for

isolated sparks), the total spark count, the pointing error, and, possibly, a pointing error flag. Only showers reasonably certain to have been contained in the chamber sensitive volume were included in the library. Showers from the $\eta \to 2\gamma$ data were assigned a pointing error from the aluminum target data on the basis of their spark count. All the information for a particular shower was used together to account for any possible correlations.

Our use of the shower library eliminated any reliance on indirect methods of calibrating the response of the spark chambers to γ-ray showers. The distributions which would have been used to determine the shower parameters became instead checks of the validity of the Monte Carlo program. It correctly predicted all distributions of shower characteristics for which comparisions were made.

3. *Event simulation*

The Monte Carlo program determined the behavior of the γ rays from the π^0 decays. For the case with Be regenerator in the decay volume, events were eliminated when a γ ray converted within the Be.

The conversion point of a γ ray which entered each spark chamber was first determined and then the shower with the closest energy was chosen from the library to represent the Monte Carlo γ ray. The shower direction was deviated from the true γ-ray direction by a polar angle equal to the pointing error and by a random azimuthal angle. A 20° half-angle cone was constructed about each shower direction with its apex at the conversion point. If the conversion point of any other γ ray fell within such a cone, its spark count was added in, but it was not counted as a separately identified shower. Because of the typically large spatial separation of the showers, the results are insensitive to the exact cone angle; changing it from 20° to 0° decreased the $3\pi^0$, four-shower fraction from 12% to 11%. The shower patterns were overlaid upon the geometry of the spark-chamber array with their dimensions adjusted for the various materials (aluminum plates, lead plates, and trigger counters) to allow for efficiency losses due to purely structural features and, if necessary, to generate a spark-count error flag. The overlays were also used to determine whether or not an event would register in the appropriate combination of scintillator-Čerenkov trigger counters to generate a chamber trigger pulse, or if the event would be vetoed by the R_1–R_6 counters.

Experimental information on the response of the SC trigger counters and tunnel shower counter to γ-ray showers was not available. Consequently, we constructed efficiency functions for use in the Monte Carlo program. The results of the experiment were found to be insensitive to the assumed efficiencies of these counters.

The efficiency function for the Čerenkov trigger counters was constructed with the aid of calibration data taken for cosmic rays traversing the counter at normal incidence. For the 3.8-cm-thick Lucite slabs used in the experiment the efficiency was 95 to 97%. Similar measurements for Lucite slabs 2.5 cm and 1.3 cm thick gave efficiencies of 93% and 71%, respectively. The efficiency function used in the Monte Carlo program was taken to be zero for zero path length and was increased linearly until an efficiency of one was reached for a path length of 2.5 cm. The sensitivity of the program to changes in the assumed efficiency was determined by a test made with two widely variant efficiency functions: The first was unity for any nonzero path length in the counter, the second was zero for path lengths below 2.5 cm and increased linearly until an efficiency of one was reached at 3.8 cm. The variation in the calculated relative detection efficiencies for $2\pi^0$ and $3\pi^0$ decays was less than 1%.

There were no calibration data available for the tunnel shower counter. The conversion points of γ rays which entered the tunnel counter were calculated from pair-creation and Compton cross sections.[10] The efficiency for detecting the γ-ray shower was taken to be equal to $0.98\ (1 - e^{(7-E)/10})$ for γ-ray energies, E in MeV, above 7 MeV and zero for energies below 7 MeV.

While the tunnel counter was important in improving the statistical accuracy of the experiment by reducing the confusable $3\pi^0$ background with four showers appearing in the chambers, its efficiency did not enter directly into the calculation of the $2\pi^0$ rate. $K_L^0 \to 2\pi^0$ decays were required to send all four γ rays into the spark chambers and thus their detection was completely independent of the tunnel efficiency. $K_L^0 \to 3\pi^0$ decays that triggered the chambers made three or more showers in the chambers with an efficiency of nearly unity. Since this was the only requirement for their detection, the tunnel counter was ignored in counting K_L^0 decays for normalization purposes. Thus the only possible influence of the efficiency was through its effect on the shape of the $3\pi^0$ background which produced four showers in the spark chambers and no tunnel shower counts. Monte Carlo $3\pi^0$ events with four visible showers and one tunnel shower count were analyzed and found to have nearly the same shape as four-shower $3\pi^0$ events with no tunnel shower counts. Hence the

over-all effect of the assumed tunnel efficiency on the calculation of the $2\pi^0$ rate was completely negligible.

The conversion points, shower directions, spark counts, and flags for the Monte Carlo events were used to make tapes similar to those for the data. Both Monte Carlo events and data were reconstructed from the γ-ray showers by essentially identical computer programs. Comparisons of Monte Carlo events to data were made only for events whose reconstructed decay points were in the fiducial volume.

C. Normalization

The fiducial volume cut was applied to the $2\pi^0$ candidates (four-shower events with no tunnel count) on the basis of the trial decay point used as the central starting point in the search procedure discussed in Sec. IV C. The fraction of $3\pi^0$ events in the fiducial volume was determined by measuring all observed K_L^0 neutral decays for a 7% sample of the data. The location of the decay point was determined by the procedure used for $2\pi^0$ candidates generalized to an arbitrary number of showers and, since no spark counts were available, with all showers given equal weight. A Monte Carlo calculation showed that the two reconstruction techniques differed by 4% in correctly determining whether the decay point was within the fiducial volume. Correcting for this difference and using the fractions determined for three-, four-, five- and six-shower events, the total number of observed K_L^0 neutral decays in the fiducial volume was calculated to be 25 845.

D. Tests of the Monte Carlo program

The Monte Carlo program was checked by comparing its predictions of distributions of observable quantities to the data and was found to be in good agreement for all but three of the comparisons made. These three are discussed in Sec. V G.

The expected shower multiplicity for the $3\pi^0$ background provided a sensitive check of the library of shower case histories as well as testing the allowance made in the program for inactive areas of the spark chamber array. Figure 9 shows that the Monte Carlo prediction of the $3\pi^0$ multiplicities agreed with the data within the accuracy (about 4%) with which a shower multiplicity could be unambiguously assigned to an event. This also indirectly checked the accuracy of the calculation of $s_2 f_2$ since the predicted shower multiplicities for both $2\pi^0$ and $3\pi^0$ events depend on the shower library and the calculated geometric inefficiencies in the spark chamber array in nearly the same way. In fact, the predictions for $2\pi^0$ decay multiplicities should be even more accurate since this mode produces fewer, but more energetic, γ rays.

The accuracy of the assignment of pointing errors to the showers was checked by comparing the distribution of apparent pointing errors obtained for Monte Carlo four-shower events to the distribution obtained for the four-shower data. The deviations were taken from the decay point deduced using the shower directions and hence were generally smaller than the deviations expected from the true decay point. The agreement between the Monte Carlo events and the data is shown in Fig. 10.

The Monte Carlo calculation of the conversion probabilities of γ rays which entered the spark chambers was checked by comparing the distributions of the depth in the chamber at which the first spark of the shower appeared for Monte Carlo events and data. The Monte Carlo prediction agreed well with the data (as shown in Fig. 11) except for the third and fourth gaps of the downstream chamber. The third gap was inoperative for part of the run, so some initial points in the data were one gap deeper in the chamber. The low probability for γ-ray leakage through the chambers is indicated by the absence of conversion points in the outer third of the chambers. The depth distributions were not separately normalized so the agreement in both side and downstream chambers indicates that the Monte Carlo program also correctly predicted the fraction of γ rays entering the different chambers.

The comparison of the distributions of γ-ray directions in four-shower events is shown in Figs. 12 and 13. The γ-ray directions were expressed

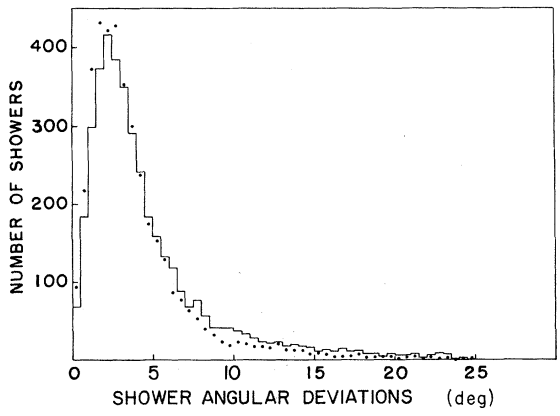

FIG. 10. Distribution of shower pointing errors in four-shower events as determined from the four-shower vertex. The points are the Monte Carlo prediction.

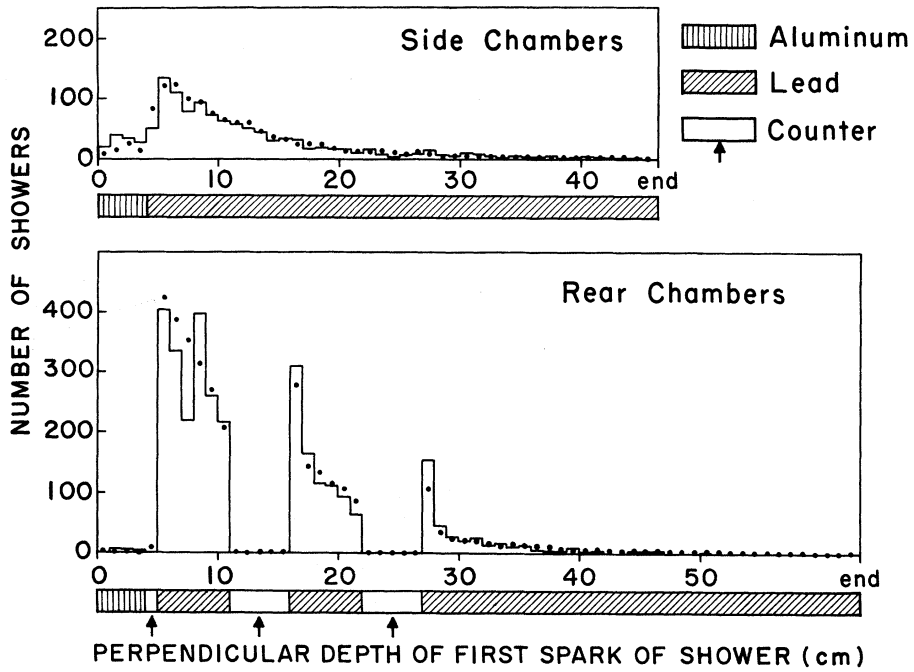

FIG. 11. Distributions for four-shower events of the perpendicular depth in the chambers at which the first spark of the shower appeared. Top drawing shows the distribution for the four side chambers. Bottom drawing shows the distribution for the downstream chamber in which two banks of trigger counters were embedded. The points are the Monte Carlo prediction.

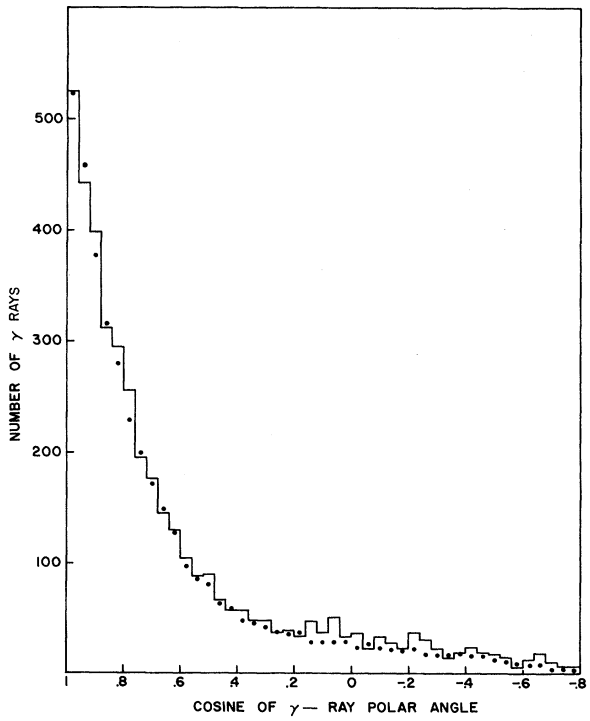

FIG. 12. Distribution of the cosine of the polar angle for γ rays in four-shower events. The points are the Monte Carlo prediction.

in a spherical coordinate system whose axis was parallel to the central trajectory of the K_L^0 beam and in which an azimuthal angle of zero corresponded to a horizontal direction. The variation with azimuthal angle was the result of the trigger requirement of two showers separated by a minimum vertical distance of 28 cm. A further check of the accuracy of the Monte Carlo calculation of the trigger requirement was provided by the distribution of the locations of the deduced decay points for four-shower events. The agreement between the Monte Carlo prediction and the data for the distribution of decay points in the direction along the K_L^0 beam is shown in Fig. 14.

In addition we investigated other ways in which the Monte Carlo program could give erroneous results.

In our apparatus the top and bottom members of the bank of R counters used to veto events with charged particles passing through the downstream chamber were shadowed by the spark chambers which formed the sides of the chamber array (see Fig. 4). γ rays which enter a side chamber obliquely can form showers which continue out the side of the chamber into the top or bottom R counter. This is an effect which cancels otherwise valid triggers and, if not properly accounted for in the Monte Carlo program, may lead to an

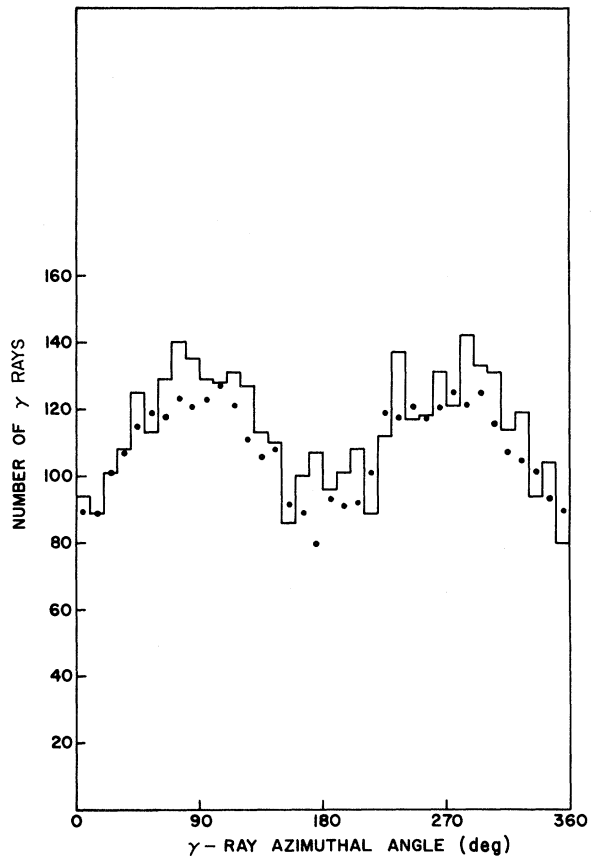

FIG. 13. Distribution of the azimuthal angle of γ rays in four-shower events. The points are the Monte Carlo prediction.

erroneous calculation of t_2 and t_3. We took a sample of data with the top and bottom R counters removed from the anticoincidence. The yield of K_L^0 events per beam monitor count was found to increase by $(12 \pm 2)\%$. The Monte Carlo program predicted the yield would increase by 13%.

In forming the shower case histories the pattern of the shower was projected on the initial direction of the shower. If the lateral spread of the showers is an important consideration in determining whether S and C will count then there could be an error in our calculation of t_2 and t_3. The data were examined to see if the events which did trigger would have been predicted as triggers by the Monte Carlo program. This study was made for a sample of $3\pi^0$ events and also for a sample of events rich in $2\pi^0$ decays [those in Fig. 19(b) with $M > 450$ MeV]. In the $3\pi^0$ sample $(5 \pm 1)\%$ of the events would have failed to have been calculated as triggers by the Monte Carlo program because of the one-dimensional representations of the showers. The corresponding result for the $2\pi^0$ sample was a failure rate of $(4 \pm 2)\%$. An additional consideration is the assumption made in the Monte Carlo program that track segments too short to make more than one spark do not contribute to the triggering. The effect of this assumption is harder to evaluate since in the data it is not possible to distinguish between such a trigger and one by a longer segment still wholly contained in the trigger counter which the Monte Carlo program will correctly predict; either one produces an event with a counter identification

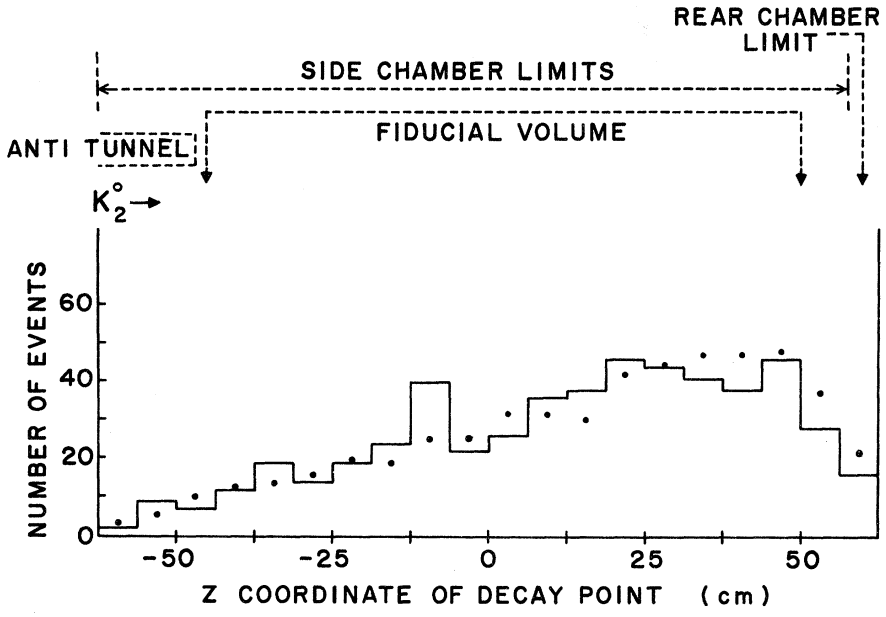

FIG. 14. Distribution along the direction of the K_L^0 beam of decay points deduced for four-shower events.

light on but with no visible associated track. Depending on the fraction of the former type, the Monte Carlo prediction will be low by an additional 0 to $3 \pm 1\%$ for the $3\pi^0$ sample and 0 to $1 \pm 1\%$ for the $2\pi^0$ sample. The events which are predicted to trigger by the Monte Carlo program but fail to trigger in the data because of lateral spreading of showers need also to be considered. A sample of data was taken with a less restrictive trigger requirement than the one described in Sec. III C. γ-ray showers were required in two SC counters separated by a minimum of only one counter rather than the usual separation requirement of two counters. Of the 119 K_L^0 decays detected with this trigger, 92 would also have triggered under the normal requirements. None of the remaining 27 events which just missed triggering normally would have been predicted as triggers by the Monte Carlo program. Consequently, to correct for simplifications made in the shower patterns in constructing the shower case histories, we raise the Monte Carlo calculated values of t_2 and t_3 by $(4+0.5)\%$ and $(5+1.5)\%$, respectively, and add 3% to the systematic error in t_3/t_2.

The value of $t_3 s_3 f_3$ predicted by the Monte Carlo program was checked by calculating the expected yield of K_L^0 decays in the fiducial volume from the observed number of beam particles which entered the liquid hydrogen target. The fraction of beam particles which were pions was well known (see Sec. III A). The number of K_L^0 mesons which emerge from the target in the solid angle which intersected our detection apparatus was calculated from the well-known production cross section for $\pi^- p \to \Lambda^0 K^0$. This calculation took into account the effect of ionization energy loss by the pions and the effect of nuclear absorption of both pions and K_L^0's in the liquid hydrogen. The principal limitation on this check was the uncertainty in the amount the K_L^0 beam was attenuated in passing through the 10.2-cm-thick lead filter. The only information available on the absorption in lead of K_L^0's in our momentum range was our own data taken early in the run for the purpose of optimizing the thickness of the lead filter. Data taken for lead thicknesses of 8.9, 10.2, and 14.0 cm gave a value of 0.34 ± 0.06 for the transmission through 10.2 cm of lead. The yield of $K_L^0 \to 3\pi^0$ decays which trigger and are reconstructed to have occurred in the fiducial volume was calculated by the Monte Carlo method and then was corrected for the errors due to the one-dimensional shower approximation. The result $(14.7 \pm 3.5) \times 10^{-9}$ $K_L^0 \to 3\pi^0$ per beam monitor count is in reasonable agreement with the observed yield of $(10.1 \pm 0.6) \times 10^{-9}$ for a sample of data taken at a low beam rate (30% of normal) to ensure a high efficiency for the electronic circuitry.

We estimate the errors in t_3/t_2 and $s_2 f_2$ to be less than 5% and 4%, respectively, and assign an over-all error of 7% to $(t_3 s_3 f_3 / t_2 s_2 f_2)$.

E. Determination of the number of $2\pi^0$ decays

The number of $2\pi^0$ events in the free decay data was determined by using a maximum-likelihood technique which fitted all 1110 four-shower events. Both real and Monte Carlo events were binned by whether or not they had at least one solution and whether the best solution had a χ^2 less than 12. The latter were further binned by mass and momentum calculated in the analysis program and by total spark-count energy.

A correction was made for background generated in the air-filled decay volume. This correction was deduced from data taken with five beryllium slabs (91 cm high by 89 cm wide by 2.5 cm thick) placed at 12.5-cm intervals in the central part of the decay volume. These data yielded a sample of 263 four-shower events reconstructed to have occurred in the fiducial volume. The beryllium four-shower events were analyzed in the same way as the four-shower events observed in air. The mass distributions calculated for these events are shown in Fig. 15.

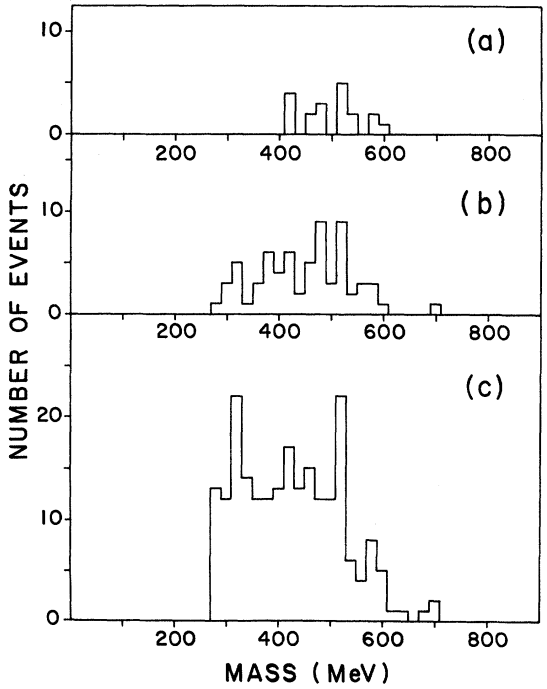

FIG. 15. Mass distributions for four-shower separated-beryllium data for (c) all events, (b) events from (c) having $\chi^2 < 12$ and $420 < P < 700$ MeV/c, and (a) events from (b) also having total P max > 175 MeV/c.

The number of four-shower events due to nuclear interactions in the air expected during the course of the run was calculated from the number observed in beryllium using the beam coincidence, M_1M_2, as a monitor. The cross section for the most important background component incoherent regeneration is given by the optical model[11,12] as

$$\sigma_{21} = |f_{21}^0|^2 \int \exp(-\tfrac{1}{3}k^2R^2\theta^2)\, d\Omega$$
$$= 3\pi |f_{21}^0|^2/(k^2R^2)\,, \qquad (5)$$

where $k = p_K/(\hbar c) = 2.69\times10^{13}$ cm^{-1}, $R = (1.1 + 1.1A^{1/3})$ F, and the forward regeneration amplitudes are $|f_{21}^0|^2 = 10.3$ F^2 (Be), 20.6 F^2 (air).[13] The ratio of expected air to beryllium events is then

$$\frac{n_{\rm air}}{n_{\rm Be}} = \left(\frac{B_{\rm air}}{B_{\rm Be}}\right)\frac{(\rho l\sigma_{21}/A)_{\rm air}}{(\rho l\sigma_{21}/A)_{\rm Be}}\left(\frac{1}{\gamma}\right)\left(\frac{I_{\rm Be}}{C_{\rm Be}+I_{\rm Be}}\right)$$
$$= (56.3)\,\frac{(1.2\times10^{-3}\times96.5\ \text{cm}\times1.88\ \text{F}^2/14.4)}{(1.848\times12.3\ \text{cm}\times1.17\ \text{F}^2/9.01)}$$
$$\times\left(\frac{1}{0.674}\right)(0.81)$$
$$= 0.346\,, \qquad (6)$$

where $B_{\rm air}$, $B_{\rm Be}$ are the number of beam monitor counts for the air and beryllium data. ρ, l, and A are the density, length in the beam direction, and atomic number, and γ is the average probability for all four γ rays from a regenerated $K_S^0 \to 2\pi^0$ decay to escape from the beryllium. The factor in the last set of parentheses is the fraction of incoherent regeneration in beryllium since coherent regeneration is essentially absent in air. The standard formulas have been numerically integrated in calculating this ratio.[14,15] The value of $B_{\rm air}$ was calculated by determining the number of M_1M_2 counts per observed K_L^0 decay for free decay data taken with a beam rate and duty cycle similar to that for the beryllium data and multiplying by the total number of K_L^0 decays observed during the entire free decay run. The distribution measured for 263 beryllium four-shower events was scaled by the above factor, 0.346, to give the expected number of confusable air background events and was added to the Monte Carlo distributions for $2\pi^0$ and $3\pi^0$ events.

The number of four-shower $K_L^0 \to 2\pi^0$ events found by the fitting program was $n_2 = 150 \pm 17$. The likelihood function was Gaussian about its maximum; the stated error was taken at the $e^{-0.5}$ points. Table II summarizes the data at various stages of analysis. The correction for the air background resulted in an $(11 \pm 3)\%$ reduction in the calculated number of $K_L^0 \to 2\pi^0$ decays in the four-shower sample. The assigned error is primarily from the statistics on the number of events (24) in the separated beryllium four-shower sample with $450 \leq M_K \leq 610$ MeV which passed the momentum and χ^2 cuts of Fig. 15(a). Should a more accurate ratio for the air/Be forward regeneration amplitudes, f_{21}^0, become available, the value for the $2\pi^0/3\pi^0$ branching ratio, R, found in this paper should be corrected to

$$R' = \frac{R}{0.89}\left(1.0 - 0.11\times\frac{10.3}{20.6}\,\frac{|f_{21}^0(\text{air})|^2}{|f_{21}^0(\text{Be})|^2}\right),$$

where we have neglected the small difference, between air and beryllium, in the angular distribution of incoherently regenerated K_S^0 mesons.

TABLE II. Neutral final-state events.

Number of	Data Free decay	Monte Carlo $2\pi^0$ fitted	Monte Carlo $3\pi^0$ fitted	Monte Carlo Sum [a]	Data Separated Be	Data Solid Be
Beam counts	2.557×10^{12}	•••	•••	•••	4.58×10^{10}	2.35×10^{11}
Spark-chamber triggers	464 000	•••	•••	•••	10 255	48 968
Events with ≥3 showers	25 845	•••	•••	•••	•••	4 126
Four-shower events in fiducial volume	1110	150	846	1110	263	732
Four-shower events with solutions	1026	149	763	1006	217	624
Four-shower events passing χ^2 b	800	141	642	847	148	451
Four-shower events passing χ^2, P	509	116	389	539	77	254
Four-shower events passing χ^2, P, E	229	87	127	227	30	133
Four-shower events passing χ^2, P, E, M	100	77	15	102	24	95
$2\pi^0$ four-shower events (calculated)	150	150	0	•••	c	244

[a] This is the sum of four-shower events generated by the Monte Carlo program for $2\pi^0$ and $3\pi^0$ decays of the K_L^0 plus air interactions which were calculated from the separated Be data by the normalization factor, $\frac{114}{263}$. This sum was constrained to give the observed number of four-shower events before cuts.

[b] The cuts are $\chi^2 < 12$, P is the momentum of the K^0 between 420 and 700 MeV/c, E is the total spark-count energy >700 MeV, and M is the invariant mass between 450 and 610 MeV/c^2.

[c] Not calculated; these 263 events are a mixture of neutron-induced and K-regeneration events and are used only for the air background correction.

F. Consideration of the decay $K_L^0 \to \pi^0\gamma\gamma$

The existence of $K_L^0 \to \pi^0\gamma\gamma$ decays might cause serious errors in our calculation of the $K_L^0 \to 2\pi^0$ rate since such events produce four-showers, conserve momentum, and have the same total spark-count energy as $2\pi^0$ events. To examine this possibility, the analysis of four-shower events was generalized so that it was valid for both $2\pi^0$ and $\pi^0\gamma\gamma$ final states. Using Monte Carlo generated $2\pi^0$, $3\pi^0$, and $\pi^0\gamma\gamma$ four-shower events the best fit as calculated on a maximum-likelihood basis gave $N_{\pi\gamma\gamma} = -12$. The upper limit on the number of $\pi^0\gamma\gamma$ events corresponding to a 90% confidence level was 25. The branching ratio corresponding to this limit was calculated to be $(K_L^0 \to \pi^0\gamma\gamma)/(K_L^0 \to 3\pi^0) < 0.0027$, which is consistent with the upper limit of 2.4×10^{-4} for this ratio.[16]

G. Test of the analysis

1. Comparison of distributions

As a test of the analysis and Monte Carlo program, the four-shower free decays and samples of known $2\pi^0$ and $3\pi^0$ four-shower events were analyzed and then compared with Monte Carlo generated distributions. The source of known $2\pi^0$ events was data taken with a 91-cm-high by 89-cm-wide by 12.3-cm-thick beryllium slab placed near the center of the decay volume. The incoherently regenerated K_S^0 mesons are produced at angles to the direction of the incident K_L^0 which are small enough that the distributions calculated by the analysis program for Monte Carlo generated coherent and incoherent $2\pi^0$ events are essentially identical. The regenerator data contained a background produced by neutron interactions in the beryllium which was easily separated by the analysis program.

A sample of fake four-shower events which were known to have come from $K_L^0 \to 3\pi^0$ decays was constructed from real five-shower events by discarding the shower with the lowest spark count. These five-shower-minus-one events were then analyzed in the same way as the four-shower data. Four-shower events were constructed from Monte Carlo five-shower events by the same process as for the data.

The fit to the mass distribution for all events, for events passing χ^2 and momentum cuts, and for events passing in addition a total spark-count energy cut, are shown in Figs. 16–18. Replacing the energy cut by one which required the maximum γ-ray transverse momentum to be greater than 175 MeV/c resulted in the distributions shown in Fig. 19. This cut is similar to the one used by Banner, Cronin, Liu, and Pilcher,[17,18] except that

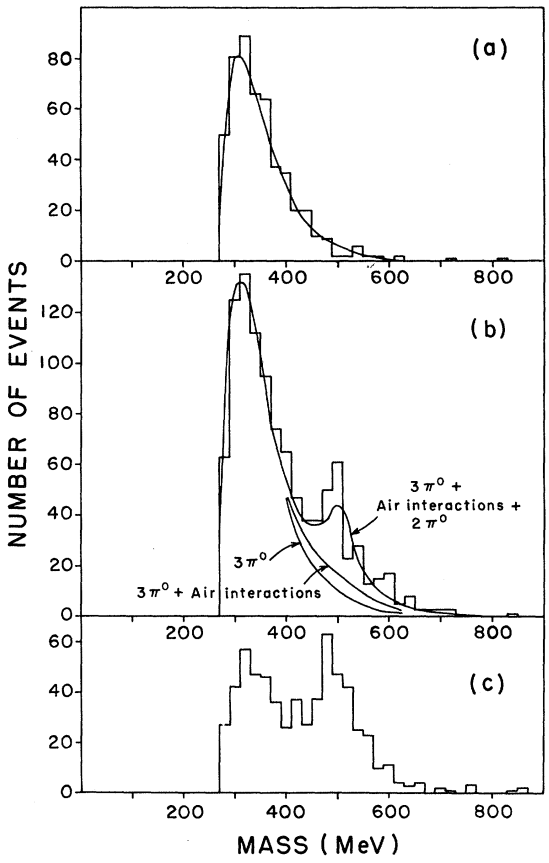

FIG. 16. Mass distributions for (a) five-shower events analyzed as four-shower events, (b) four-shower events, and (c) four-shower events from a 12.3-cm-thick beryllium regenerator

spark counting is used here for the direct measurement of the γ-ray energy. These cuts are both independent of the kinematic analysis of the event. The momentum and the total spark-count energy distributions are shown in Figs. 20 and 21.

The Monte Carlo prediction shown for each of the restricted data samples in Figs. 17–21 corresponds to the maximum-likelihood fit obtained using all of the events of each type of data, with the exception of the beryllium data. That fit was made using a restricted sample having $\chi^2 < 12$ and momentum between 420 and 700 MeV/c in which the $2\pi^0$ events were clearly separated from the neutron background. The good fits to the data for the restricted samples shown in Figs. 17–19 are further evidence that the Monte Carlo program correctly describes the data under the different cuts. The Monte Carlo prediction for the five-shower-minus-one distribution was essentially identical to the prediction for the $3\pi^0$ four-shower events.

The momentum distribution shown in Fig. 20 for

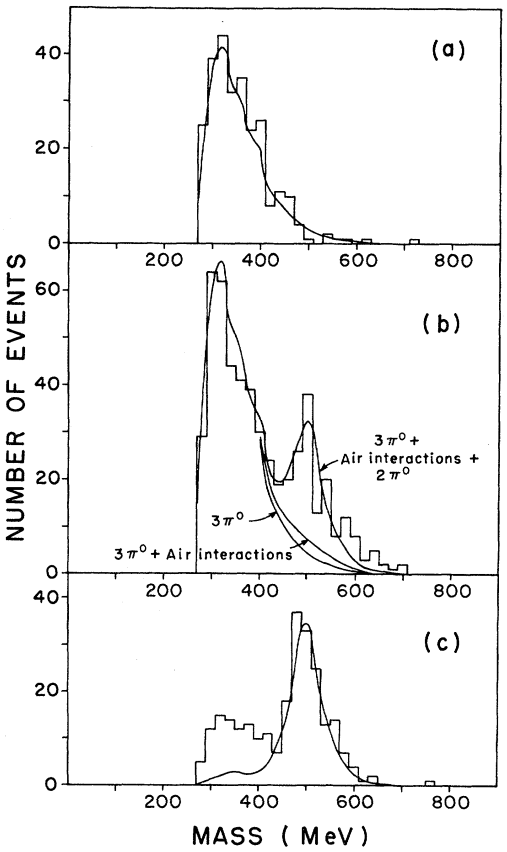

FIG. 17. Mass distributions for four-shower events calculated to have $\chi^2 < 12$ and $420 < P < 700$ MeV/c for (a) five-shower-minus-one data. (b) four-shower data, and (c) beryllium-regenerator data.

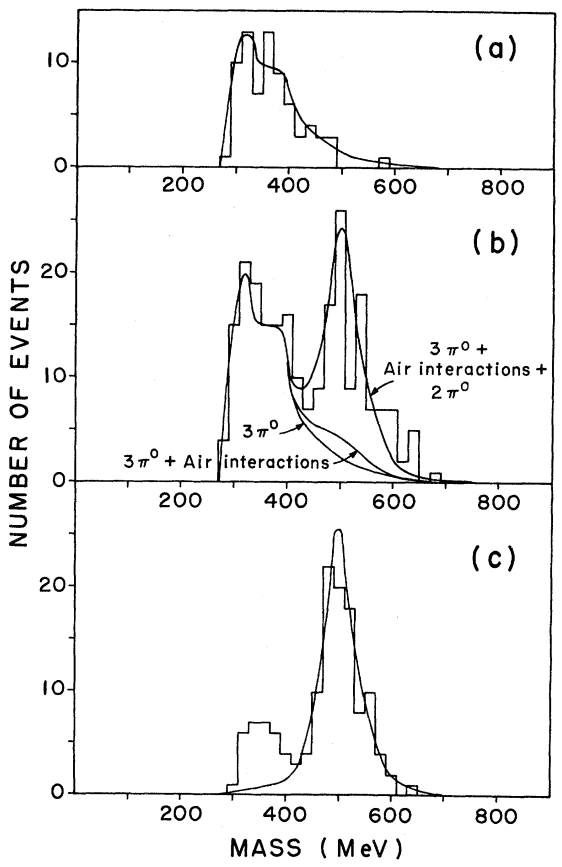

FIG. 18. Mass distributions for four-shower events calculated to have $\chi^2 < 12$, $420 < P < 700$ MeV/c, and total spark-count energy greater than 700 MeV for (a) five-shower-minus-one data, (b) four-shower data, and (c) beryllium-regenerator data.

the regenerator data is distinct from that for the five-shower-minus-one data and agrees well with that prediction using the known momentum distribution of the K_L^0 beam (shown in Fig. 3). The momentum distribution for the four-shower data shifts accordingly as the fraction of $2\pi^0$ events is enriched by selecting only those events with mass greater than 450 MeV, $\chi^2 < 12$, and total spark-count energy greater than 700 MeV.

The distributions of total spark count were expressed as energies (using the fitted curve shown in Fig. 7) so that a comparison to the known energy spectrum of the K_L^0 beam could be made. For $3\pi^0$ six-shower and $2\pi^0$ four-shower events, all of the energy of the incident K_L^0 is displayed in the showers. The distributions for these events are well centered on the K_L^0 energy spectrum shown at the bottom of Fig. 21. All distributions agree with the Monte Carlo predictions. In conclusion, the five-shower-minus-one data indicate that the distribution produced for $3\pi^0$ four-shower events is distinct from the $2\pi^0$ distribution and also is correctly described by the Monte Carlo program.

2. *Errors*

The effect on the $2\pi^0$ analysis efficiency due to uncertainties in the calibrations of shower pointing accuracy and spark counts due to the limited number of library events was determined. For spark counts above 50, the median pointing error has reached an asymptotic value of 4.3°. The uncertainty in this median value due to the limited number (94) of calibration events in this region was ±13%. The effect of this uncertainty was evaluated using Monte Carlo $2\pi^0$ events generated with pointing errors systematically altered by 13% from the values given by the shower library. The change in the efficiency (evaluated for a sample of 500 events) of the analysis program to calculate a momentum value between 420 and 700 MeV/c and a mass value greater than 450 MeV was ±2.7%.

A similar procedure was used to evaluate the effect of the uncertainty in the spark-count calibrations. The fitted curve shown in Fig. 7 was

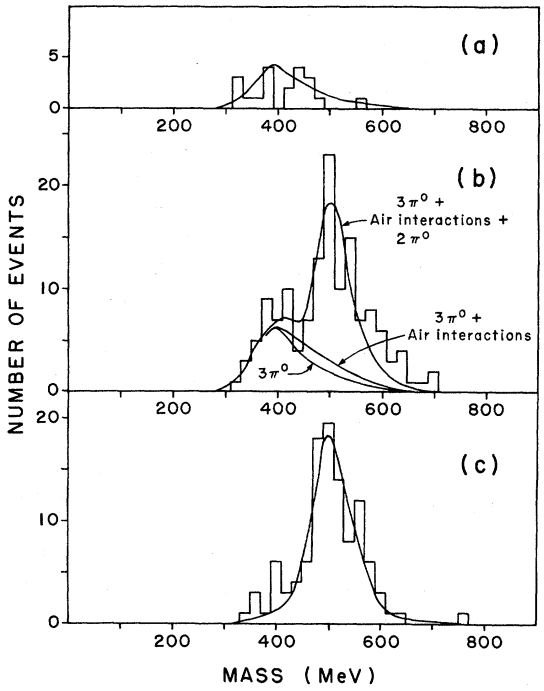

FIG. 19. Mass distributions for four-shower events calculated to have $\chi^2 < 12$, $420 < P < 700$ MeV/c, and which have a shower with momentum transverse to the direction of the K_L^0 greater than 175 MeV/c as deduced from the spark-count energy for (a) five-shower-minus-one data, (b) four-shower data, and (c) beryllium-regenerator data.

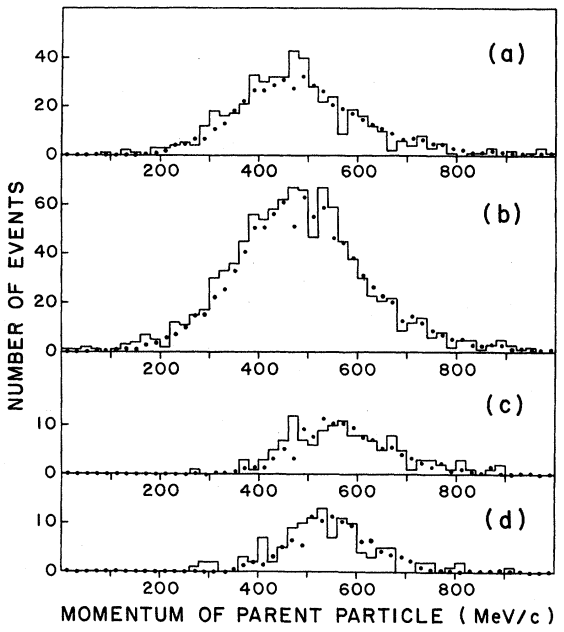

FIG. 20. Momentum distributions for (a) five-shower-minus-one data. (b) four-shower data, (c) four-shower events having $\chi^2 < 12$, $M > 450$ MeV, and total spark-count energy, E, greater than 700 MeV, and (d) beryllium-regenerator events having $\chi^2 < 12$, $M > 450$ MeV, and $E > 700$ MeV. The points are the Monte Carlo predictions.

well determined for γ-ray energies below 200 MeV because of the large number of calibration events in this region. Above 200 MeV the slope of the fitted curve was uncertain by ±10%. The effect of this uncertainty was evaluated using Monte Carlo $2\pi^0$ events generated with spark counts altered from the values given by the shower library in a way that corresponded to a change of ±10% in the slope of the spark-count curve above 200 MeV. This alteration caused a ±2.6% change in the efficiency of the analysis program to calculate a momentum value between 420 and 700 MeV/c and a mass value greater than 450 MeV for these events.

There are three disagreements between the Monte Carlo predictions and the distributions observed in the data. The first of these is that the number of free-decay four-shower events having solutions but failing the $\chi^2 < 12$ cut is larger than predicted. Specifically, referring to Table II there are 84 events with no solutions, 226 that have solutions but fail the χ^2 cut, and 800 that pass it. The Monte Carlo predictions are 104, 159, and 847, respectively. We do not understand the detailed nature of this discrepancy, but the fraction of events passing later cuts is in good agreement with the Monte Carlo predictions.

A second disagreement is that the percentage of K_L^0-decay events with tunnel counts was 32% as compared with the 18% calculated by the Monte Carlo method. After correcting the data for a 5% tunnel accidental rate, it remains 9% higher than predicted. The tunnel counter was not directly calibrated and it is probable that the Monte Carlo prediction for the tunnel counter efficiency is too low. Since this efficiency does not enter into the determination of the numbers of $2\pi^0$ or $3\pi^0$ decays and hence does not affect the $2\pi^0$ to $3\pi^0$ branching ratio, no attempt was made to adjust the Monte Carlo to fit the tunnel data.

The most serious difference is an excess of events with a mass greater than 570 MeV (see Figs. 16–19). This high-mass tail is not seen in either regenerator or five-shower-minus-one events and so represents a possible source of background that may extend under the K peak to masses as low as 480 MeV. The number in the tail is probably not a statistical fluctuation; for instance, we expect only eight events with $M > 570$ MeV to pass the momentum, spark count, and χ^2 cuts while we see 22 (there are 24 in excess when the high-transverse-momentum cut is used in place of the spark-count cut).

We examined each high-mass event in detail.

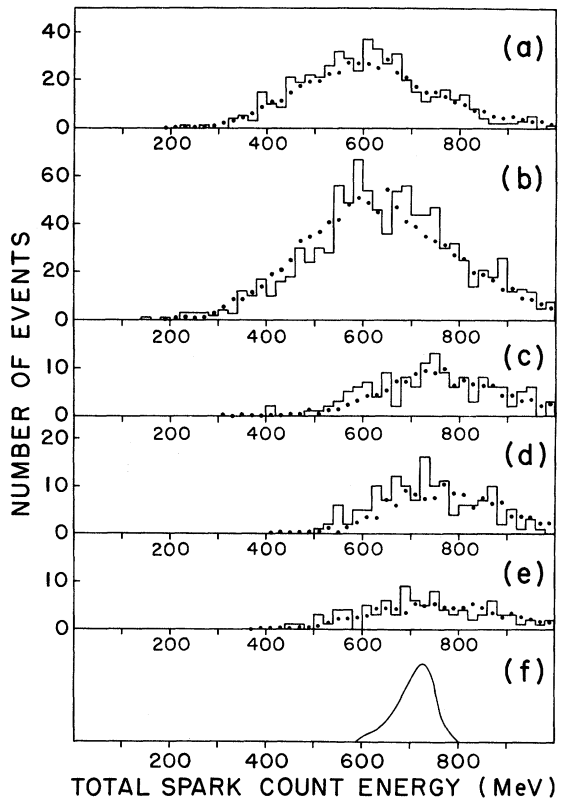

FIG. 21. Distributions of total spark-count energy for (a) five-shower-minus-one data, (b) four-shower data, (c) four-shower events having $\chi^2 < 12$, $M > 450$ MeV, and $420 < P < 700$ MeV/c, (d) beryllium-regenerator data having $\chi^2 < 12$, $M > 450$ MeV, and $420 < P < 700$ MeV/c, and (e) six-shower events. The points are the Monte Carlo predictions. The calculated energy spectrum of the K_L^0 beam is shown in (f).

One turned out to have five showers in which one lined up exactly with a second in one view and a third in the other view. The others were reasonably normal-looking events except many had a very-high-energy shower (as might be expected in such a sample). These high-mass events were distributed approximately uniformly in time during the run and their vertices were distributed uniformly throughout the decay volume. No concentration was seen near the edges.

The search for possible $K_L^0 \to \pi^0\gamma\gamma$ events was motivated by this unexplained excess at high mass. As has been mentioned in subsection F, no such events were found. Under the $\pi^0\gamma\gamma$ analysis, 13 of the 24 high-mass events passing the χ^2, momentum, and perpendicular momentum cuts had a $\gamma\gamma$ mass in a peak near the π^0 mass. This is not unreasonable for a predominantly $2\pi^0$ sample, considering the rather poor pairing efficiency of the $\pi^0\gamma\gamma$ analysis. Seven of the nine events in this sample with especially high-spark-count showers (450 MeV) were in the π^0 peak.

An event-by-event comparison in the high-mass region was made with the measurements previously used in Ref. 19. These measurements, which showed no high-mass tail and in which the K peak was 20 MeV low, had used a linear spark-count conversion which we now know to be valid only for $E_\gamma < 200$ MeV. The present spark-count conversion increases the average energy per shower by 46 MeV. The highest energy shower of each event increases by an average of 188 MeV. As a result 86% of the new measurements showed an increase of 25 MeV or more in mass, with little change in photon pairing. Thus the difference between the measurements does seem related to the change in spark-count conversion. However, the regenerator events do not have such an excess of events at high mass, which would indicate that the high-mass tail is not caused by a possible error in the spark-count conversion. Because of this ambiguity we consider the origin of the excess to be uncertain.

Explanations involving nuclear reactions from background radiation in the decay volume also seem unlikely because of the lack of a similar excess in the regenerator data. Furthermore, the excess in free decay cannot be neutrons produced by the π^- beam in the hydrogen target since the maximum energy neutron can produce a $2\pi^0$ state of mass no greater than about 470 MeV.

While as much as one-third to one-half of the excess of 14 events might be due to a statistical fluctuation, the most conservative estimate of the error is to assume that it is entirely systematic. Perhaps all of the excess may be $K_L^0 \to 2\pi^0$ with a mass calculated too high due to fluctuations in chamber operation or a shift in spark counting for those events. If the calculated mass for these 14 events is shifted lower by 40 MeV, the fitted number of $2\pi^0$ events before cuts, n_2, increases from 150 to 166 events. On the other hand, the excess may be due to some unknown background which should be subtracted from the data. If we assume that the mass distribution of this background is not peaked under the K_L^0 peak but starts at zero at 480 MeV, increases linearly to the observed level of excess at 570 MeV, and follows the excess thereafter, the resultant fitted value of n_2 decreases from 150 to 134 events.

Guided by these variations we assign a systematic error to n_2 of ± 16 events. Combining this error with the other statistical errors results in

$$n_2 = (150 \pm 17)(1 \pm 0.027)(1 \pm 0.026) \pm 16$$

$$= 150 \pm 18 \text{ (stat)} \pm 16 \text{ (syst)} .$$

VI. RESULTS

A. Calculation of relative rates $(K_L^0 \to 2\pi^0)/(K_L^0 \to 3\pi^0)$

To calculate the relative decay rate, R, from Eq. (3), we need

$$\frac{D_3}{D_2}\frac{t_3 s_3 f_3}{t_2 s_2 f_2} = 0.988 \times \frac{0.212 \times 0.999 \times 0.839}{0.156 \times 0.672 \times 0.870} \times (1 \pm 0.07) = 1.90 \pm 0.13 \quad (7)$$

from the Monte Carlo program (see Sec. V B). The correction factor for accidentals, $a_2 = 0.91 \pm 0.01$, is deduced from the random trigger data in Table I, which gives accidental spark chamber shower and tunnel counter rates for low and high beam intensities. The appropriate accidental rates are weighted proportionally to the total numbers of K_L^0 events observed at the various intensities. The uncertainty is due to the limited sample (2000 frames) of randomly triggered data. We determined $n_3 = 25\,845 \times (1 \pm 0.017)$ from the total number of observed K_L^0 events as described in Sec. V C, where the uncertainty is due to the limited number of such events measured for the fiducial volume correction. Finally,

$$R = \frac{D_3 t_3 s_3 f_3}{D_2 t_2 s_2 f_2}\frac{1}{a_2}\frac{n_2}{n_3} = (1.90 \pm 0.13)(0.91 \pm 0.01)^{-1}\frac{(150 \pm 18 \pm 16)}{(25\,845)(1 \pm 0.017)} = 0.0121 \pm 0.0017\ (\text{stat}) \pm 0.0013\ (\text{syst})\ . \quad (8)$$

B. Alternative methods of normalization—regenerator

The normalization of $2\pi^0$ to $3\pi^0$ events in the same film avoided the need to know the relative K_L flux but required knowledge of the relative trigger efficiencies and the absolute $2\pi^0 \to$ four-shower and analysis efficiencies. We can also normalize to the regenerator data that was used in testing the Monte Carlo. The Monte Carlo curve, fitted to the regenerator data in Figs. 17(c) to 19(c), corresponds to 244 regenerated four-shower events. The relative K fluxes are easily found from the beam monitor counts and except for a small decrease in analysis efficiency from nonzero degree incoherent regeneration events, the trigger and analysis efficiencies are identical. A correction must be made for absorption of γ rays in the regenerator, but this can be accurately calculated. The main uncertainty is in the knowledge of f_{21}^0. The number of regenerator $2\pi^0$ four-shower events, n_{Be}, and the corresponding number for free decay, n_2, are given by

$$n_{\text{Be}} = B_{\text{Be}} K_L [r_{\text{coh}} R_S D_2 (\gamma t_2 s_2 f_2)_{\text{coh}} (a_2)_{\text{Be}} + r_{\text{incoh}} R_S D_2 (\gamma t_2 s_2 f_2)_{\text{incoh}} (a_2)_{\text{Be}}]\ , \quad (9)$$

$$n_2 = B_{\text{free}} K_L \langle 1 - \exp(-z/\eta c\tau)\rangle \times [R_L D_2 (t_2 s_2 f_2 a_2)_{\text{free}}]\ , \quad (10)$$

where

B = number of beam monitor counts,

K_L = number of K_L^0 mesons incident per beam count,

$r_{\text{coh, incoh}}$ = number of $K_L^0 \to K_S^0$ from coherent or incoherent regeneration per incident K_L^0, including interference effects,

$R_{S,L}$ = branching ratio of $(K_{S,L}^0 \to 2\pi^0)/(K_{S,L}^0 \to \text{all})$,

D_2 = probability that neither pion undergoes a Dalitz decay,

γ = probability that all four decay γ rays escape from the beryllium, $(t_2 s_2 f_2)_{\text{coh, incoh, free}}$ = product of trigger, four-shower, and fiducial volume reconstruction efficiencies for coherent, incoherent, or free decay events,

$(a_2)_{\text{Be, free}}$ = probability that the event is not rejected due to an accidental tunnel count or fifth shower for regnerator or free decay event (see Table I).

$\langle 1 - \exp(-z/\eta c\tau)\rangle$ = average K_L^0 decay probability within the Monte Carlo generating volume used for $(t_2 s_2 f_2)_{\text{free}}$.

The expressions for r_{coh} (see Ref. 11) and r_{incoh} (see Ref. 12) were evaluated in short steps throughout and downstream of the regenerator and the resulting decay intensities used as input to the Monte Carlo program. Interference between CP violation and coherent regeneration has been included using our value of η_{00}, but it had a negligible effect on r_{coh}, which itself is only a quarter of the total rate. While f_{21}^0 is the main parameter to which the regeneration results are sensitive, we list here for completeness the other nuclear parameters used in this calculation as well:

$|f_{21}^0| = 3.12$ F

$|f_{22}^0| = 4.08$ F

$\phi_{21}^0 - \phi_{00} = -43^\circ - 23^\circ = -66^\circ$

R_{Be} = radius (Be) = 3.42 F

σ_T = total cross section, K_L^0 on Be = 180 mb.

Combining (9) and (10) to eliminate K_L, we have

$$R_L = \frac{B_{\text{Be}}}{B_{\text{free}}} \times \frac{r_{\text{coh}}(\gamma t_2 s_2 f_2)_{\text{coh}} + r_{\text{incoh}}(\gamma t_2 s_2 f_2)_{\text{incoh}}}{\langle 1 - \exp(-z/\eta c\tau)\rangle (t_2 s_2 f_2)_{\text{free}}} \times \frac{(a_2)_{\text{Be}}}{(a_2)_{\text{free}}} \times \frac{n_2}{n_{\text{Be}}} \times R_S$$

$$= 0.092 \times \frac{[(0.0052)(776/10^4) + (0.0162)(585/9193)]}{\langle 1 - \exp(-119.4/1653)\rangle (1760/20\,000)} \times \frac{0.85}{0.91} \times \frac{(150 \pm 33)}{(244 \pm 16)} \times 0.3123\ , \quad (11)$$

or

$$R_L = (3.87 \pm 0.95) \times 10^{-3} \times |f_{21}^0/3.12\ \mathrm{F}|^2 , \tag{12}$$

where the explicit dependence on f_{21}^0 is retained and where the indicated error is the sum of the statistical and systematic errors. Finally, dividing by the ratio $(K_L^0 \to 3\pi^0)/(K_L^0 \to \text{all})$, we have for R, the $(K_L^0 \to 2\pi^0)/(K_L^0 \to 3\pi^0)$ ratio,

$$R = (0.018 \pm 0.005) \times |f_{21}^0/3.12\ \mathrm{F}|^2 .$$

C. K_L charged-decay normalization

As an additional check, the charged-decay data were used to normalize the K_L flux to the beam monitor, M_{12}. The film for the charged runs was scanned and 1812 charged K decays were found in the fiducial volume. A Monte Carlo program was used to determine the trigger efficiency, t_c for each of the decays to $\pi e \nu$, $\pi \mu \nu$, and $\pi^+\pi^-\pi^0$. The number of charged decays, n_c, which occur in the fiducial volume is given by

$$n_c = B_c K_L \langle 1 - \exp(-z/\eta c\tau) \rangle \left[(R_c t_c f_c)_{\pi e \nu} + (R_c t_c f_c)_{\pi \mu \nu} + (R_c t_c f_c)_{\pi^+\pi^-\pi^0} \right] , \tag{13}$$

where B_c is the number of beam monitor counts for the charged runs, R_c is the branching ratio for each decay mode, and where t_c and f_c are the corresponding trigger efficiencies and fiducial volume corrections. Combining Eqs. (10) and (13) to eliminate the K_L^0 flux, we have

$$\frac{R_L}{R_c} = \frac{B_c}{B_{\text{free}}} \frac{t_c f_c}{D_2 t_2 s_2 f_2 a_2} \frac{n_2}{n_c}$$

$$= \frac{60.5}{2557} \frac{(0.123 \pm 0.009)(150 \pm 17 \pm 16)}{(0.976)(0.091 \pm 0.009)(0.91 \pm 0.01)(1812 \pm 60)}$$

$$= 0.0030 \pm 0.0005\ (\text{stat}) \pm 0.0003\ (\text{syst}) ,$$

where R_c and $t_c f_c$ apply to the sum of all charged decay modes. The product of this ratio and the ratio of charged to $3\pi^0$ decay rates, $R_c/R_3 = 0.796/0.213$, gives the ratio of $2\pi^0$ to $3\pi^0$ rates, $R = (0.0112 \pm 0.0031)$. This is in agreement with the direct normalization to $3\pi^0$ decays and indicates that the Monte Carlo calculation of the absolute $3\pi^0$ detection efficiency is reasonably accurate.

D. Conclusion

We have determined the value for the $(K_L^0 \to 2\pi^0)/(K_L^0 \to 3\pi^0)$ branching ratio, R, using three separate normalizations: $3\pi^0$ decays, regeneration in beryllium, and K_L^0 charged decay modes. In order to calculate the absolute square of the parameter $\eta_{00} = A(K_L \to 2\pi^0)/A(K_S \to 2\pi^0)$, we choose the $3\pi^0$ normalization as the most accurate and the one with the lowest probable systematic error. Using the known values for the $K_S^0 \to 2\pi^0$ and $K_L \to 3\pi^0$ decay rates[16] we find

$$|\eta_{00}|^2 = [14.1 \pm 1.9\ (\text{stat}) \pm 1.5\ (\text{syst})] \times 10^{-6} ,$$

where the statistical and systematic errors are to be added.

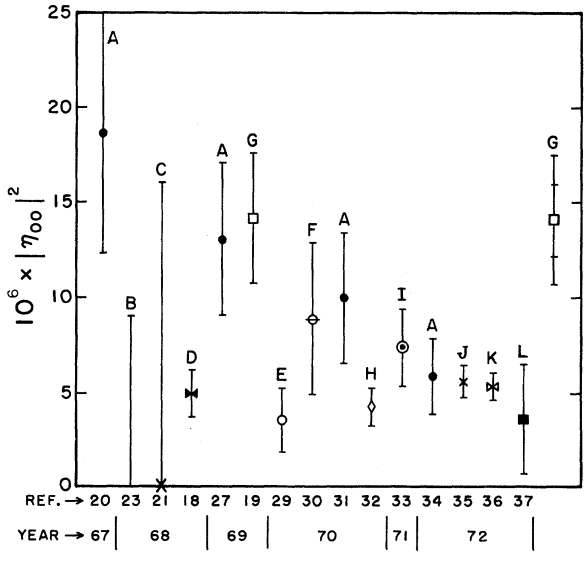

FIG. 22. Values for $|\eta_{00}|^2$ from various experiments ordered chronologically by date of publication. Each letter corresponds to the particular experiment listed in Table III. The points J and K have been calculated using the new (higher) values for $|\eta_{+-}|$.

TABLE III. Other results for $|\eta_{00}|$.

Experiment	Reference	Detector	Normalization	$10^3\times\|\eta_{00}\|$
A CERN-RHEL-Aachen	20	OSC	C regen	$4.3^{+1}_{-0.8}$
	27		C regen	3.6 ± 0.6
	31		$3\pi^0$	3.2 ± 0.5
	34		C regen	2.4 ± 0.5
B Princeton I	22, 23	OSC		< 3.0 at 90% CL
C Princeton II	21, 24	OSC	$3\pi^0$	< 4.0
D Princeton II	17, 18, 25	OSC	$3\pi^0$	2.2 ± 0.3
E CERN-Orsay-École Polytechnique	26, 29	HLBC	$3\pi^0$	1.9 ± 0.5
F CERN	28, 30	OSC	Cu regen	2.96 ± 0.70
G Berkeley-Hawaii	19	OSC	$3\pi^0$	3.7 ± 0.5
H Moscow-Dubna	32	HLBC	$3\pi^0$	2.02 ± 0.23
I Orsay-CERN	33	OSC	Cu regen	2.71 ± 0.37
J Princeton II	35	WSC	$K_L\to\pi^+\pi^-$	$(1.03\pm 0.07)\times\|\eta_{+-}\|$
K Aachen-CERN-Torino	36	WSC	$3\pi^0$	$(1.0\pm 0.06)\times\|\eta_{+-}\|$
L SLAC	37	WSC	$3\pi^0$	$1.9^{+0.7}_{-1.1}$

Our result is compared with those of other experiments[17-37] in Fig. 22. For each of these experiments the method of normalization, type of detector, and the reference are listed in Table III. Our preliminary value[19] differed from the world average by 3.5 standard deviations. Our final value is not substantially different, although it is based on the complete data sample and a different method of analysis. Since the current world average is dominated by experiments that are normalized directly to the $K_L^0\to\pi^+\pi^-$ rate, we need the latter to complete the comparison. The four most recent measurements of $K_L^0\to\pi^+\pi^-$ have small quoted errors and give a value for the decay rate that is over 11 standard deviations above the former world average.[38] If the new value is used our final result for $|\eta_{00}|^2$ is about three standard deviations above the average of the other experiments listed.

ACKNOWLEDGMENTS

We deeply appreciate the efforts of D. O. Caldwell, R. B. Chaffee, D. I. Cheng, R. D. Eandi, and J. E. Nelson in the early stages of the experiment, and wish to thank L. Shiraishi and J. Wilson for their help in the data analysis. We are grateful to A. C. Helmholz and J. A. Poirier for their interest and support.

*Research supported in part by the National Science Foundation.

†Present address: Rutherford High Energy Laboratory, Chilton, Didcot, Berkshire, England.

‡Work supported by the United States Atomic Energy Commission.

§Present address: Syracuse University, Syracuse, New York 13210.

‖Present address: University of Washington, Seattle, Washington 98105.

[1]J. H. Christenson, J. W. Cronin, V. L. Fitch, and R. Turlay, Phys. Rev. Lett. 13, 138 (1964).

[2]J. Steinberger, in Proceedings of the Topical Conference on Weak Interactions, Geneva, 1969, CERN Report No. 69-7 (unpublished).

[3]R. J. Cence *et al.*, UCRL Report No. 18368 (Rev.), 1968 (unpublished).

[4]T. B. Risser, Ph.D. thesis, UCRL Report No. 20039, 1970 (unpublished).

[5]J. C. Doyle, Ph.D. thesis, UCRL Report No. 18139, 1969 (unpublished).

[6]S. I. Parker and C. A. Rey, Nucl. Instrum. Meth. 43, 361 (1966); C. A. Rey and S. I. Parker, *ibid.* 54, 314 (1967).

[7]W. P. Oliver, Ph.D. thesis, UCRL Report No. 19397, 1967 (unpublished).

[8]I. Linscott, Ph.D. thesis, LBL Report No. 995, 1972 (unpublished).

[9]P. Heusse, B. Aubert, C. Pascaud, and J. Vialle, Lett. Nuovo Cimento 3, 449 (1970).

[10]G. W. Grodstein, NBS Circular 583, 1957 (unpublished).

[11]V. Fitch, in *Proceedings of the Second Hawaii Topical Conference on Particle Physics*, edited by S. Pakvasa and S. F. Tuan (Hawaii Univ. Press, Honolulu, Hawaii,

1968).
[12]R. H. Good, R. P. Matsen, F. Muller, O. Piccioni, W. M. Powell, H. S. White, W. B. Fowler, and R. W. Birge, Phys. Rev. 124, 1223 (1961).
[13]The factor $\frac{1}{3}$ in the angular distribution is used to fit the Gaussian to the optical model angular distribution $[J_1(kR \sin\theta)/\sin\theta]^2$. The two are indistinguishable in our experiment.
[14]J. H. Christenson, J. W. Cronin, V. L. Fitch, and R. Turlay, Phys. Rev. 140, B74 (1965), Eq. (7).
[15]See Ref. 12, Eq. (23).
[16]Particle Data Group, Rev. Mod. Phys. 45, S1 (1973).
[17]M. Banner, J. W. Cronin, J. K. Liu, and J. E. Pilcher, Phys. Rev. Lett. 21, 1107 (1968).
[18]M. Banner, J. W. Cronin, J. L. Liu, and J. E. Pilcher, Phys. Rev. 188, 2033 (1969) (final analysis of Ref. 17).
[19]R. J. Cence, B. D. Jones, V. Z. Peterson, V. J. Stenger, J. Wilson, D. I. Cheng, R. D. Eandi, R. W. Kenney, I. Linscott, W. P. Oliver, S. I. Parker, and C. A. Rey, Phys. Rev. Lett. 22, 1210 (1969).
[20]J.-M. Gaillard, F. Krienen, W. Galbraith, A. Hussri, M. R. Jane, N. H. Lipman, G. Manning, T. J. Ratcliffe, P. Day, A. G. Parham, B. T. Payne, A. C. Sherwood, H. Faissner, and H. Reithler, Phys. Rev. Lett. 18, 20 (1967).
[21]J. W. Cronin, P. F. Kunz, W. S. Risk, and P. C. Wheeler, Phys. Rev. Lett. 18, 25 (1967).
[22]T. Kamae, Ph.D. thesis, Princeton Report No. 45, 1968 (unpublished).
[23]D. F. Bartlett, R. K. Carnegie, V. L. Fitch, K. Goulianos, D. P. Hutchinson, T. Kamae, R. F. Roth, J. S. Russ, and W. Vernon, Phys. Rev. Lett. 21, 558 (1968).
[24]P. C. Wheeler, Ph.D. thesis, Princeton Report No. 47, 1968 (unpublished).
[25]J. K. Liu, Ph.D. thesis, Princeton Report No. 48, 1968 (unpublished).
[26]I. A. Budagov, D. C. Cundy, G. Myatt, F. A. Nezrick, G. H. Trilling, W. Venus, H. Yoshiki, B. Aubert, P. Heusse, I. LeDong, J. P. Lowys, D. Morellet, E. Nagy, C. Pascaud, L. Behr, P. Beillière, G. Boutang, M. Schiff and J. Vander Velde, Phys. Lett. 28B, 215 (1968).
[27]J.-M. Gaillard, W. Galbraith, A. Hussri, M. R. Jane, N. H. Lipman, G. Manning, T. J. Ratcliffe, H. Faissner, and H. Reithler, Nuovo Cimento 59A, 453 (1969) (final analysis of Ref. 20).
[28]J. C. Chollet, J.-M. Gaillard, M. R. Jane, T. J. Ratcliffe, J.-P. Repellin, K. R. Schubert, and B. Wolff, CERN Report No. 69-7, 309, 1969 (unpublished).
[29]I. A. Budagov, D. C. Cundy, G. Myatt, F. A. Nezrick, G. H. Trilling, W. Venus, H. Yoshiki, B. Aubert, P. Heusse, I. LeDong, J. P. Lowys, D. Morellet, E. Nagy, C. Pascaud, L. Behr, P. Beillière, G. Boutang, and M. Schiff, Phys. Rev. D 5, 815 (1970) (final analysis of Ref. 26).
[30]J. C. Chollet, J.-M. Gaillard, M. R. Jane, T. J. Ratcliffe, J.-P. Repellin, K. R. Schubert, and B. Wolff, Phys. Lett. 31B, 658 (1970).
[31]H. Faissner, H. Reithler, W. Thomé, J.-M. Gaillard, W. Galbraith, M. R. Jane, N. H. Lipman, and G. Manning, Nuovo Cimento 70A, 57 (1970) (uses data of Refs. 20 and 27).
[32]V. V. Barmin, V. G. Barylov, V. S. Borisov, G. K. Bysheva, G. S. Veselovsky, V. M. Golubchikov, L. L. Goldin, G. V. Davidenko, A. G. Dolgolenko, V. S. Demidov, N. K. Zombkovskaya, L. N. Kondratiev, N. S. Konoplev, A. G. Meshkovsky, G. S. Mirosidi, G. K. Tumanov, T. A. Chistyakova, I. V. Chuvilo, V. A. Shebanov, E. M. Bogdanovicz, V. B. Vinogradov, I. A. Ivanovskaya, T. I. Kanarek, V. A. Maximenko, Z. I. Ogrzevalski, L. S. Okhrimenko, and Z. S. Strugalski, Phys. Lett. 33B, 377 (1970).
[33]B. Wolff, J. C. Chollet, J.-P. Repellin, J.-M. Gaillard, M. R. Jane, and K. R. Schubert, Phys. Lett. 36B, 517 (1971) (continuation of Ref. 30).
[34]U. Heeren, Nuovo Cimento 11A, 305 (1972) (uses data of Refs. 20 and 27).
[35]M. Banner, J. W. Cronin, C. M. Hoffman, B. C. Knapp, and M. J. Shochet, Phys. Rev. Lett. 28, 1597 (1972).
[36]M. Holder, E. Radermacher, A. Staude, P. Darriulat, J. Deutsch, M. Hansroul, S. Orito, J. Pilcher, C. Rubbia, P. Strolin, K. Tittel, A. Fainberg, C. Grosso-Pilcher, and M. Scire, Phys. Lett. 40B, 141 (1972).
[37]G. Akavia, R. Coombes, D. Dorfan, J. Enstrom, D. Fryberger, R. Piccioni, D. Porat, D. Raymond, K. Riley, A. Rothenberg, H. Saal, M. Schwartz, and S. Wojcicki, SLAC Report No. 145, 1972 (unpublished).
[38]D. R. Nygren, LBL Report No. 2407, 1973 (unpublished).